SPE
Society of Petroleum Engineers

SPE 22921

APPLICATION OF A GENERAL MATERIAL BALANCE FOR HIGH-PRESSURE GAS RESERVOIRS

by M. J. Fetkovich, D. E. Reese, and C. H. Whitson, Phillips Petroleum Co.

SPE Members

Abstract

This paper presents the derivation of a general gas material balance that has particular application to high pressure gas reservoirs. The material balance is valid for both normal-pressure and over-pressured (geo-pressured) reservoirs. Its main application is to calculate original gas in place and assist in calculating remaining recoverable reserves from pressure-production data.

The form of the material balance equation is

$$(p/z)[1-\bar{c}_e(p)(p_i-p)] = (p/z)_i(1-G_p/G) \quad \ldots\ldots\ldots\ldots\ldots (1)$$

which includes a pressure-dependent cumulative effective compressibility term $\bar{c}_e(p)$ that is defined in terms of the following reservoir parameters: (1) pore compressibility, (2) water compressibility, (3) gas solubility, and (4) total water associated with the gas reservoir volume. "Associated" water includes connate water, water within interbedded shales and non-pay reservoir rock, and any limited aquifer volume. $\bar{c}_e$ physically represents the cumulative change in hydrocarbon pore volume caused by compressibility effects and encroaching water.

High pressure gas reservoirs typically have curved p/z-G_p plots (concave downward). Incorrect extrapolation of early data may result in serious overestimation of original gas in place and remaining recoverable reserves. The proposed form of the gas material balance equation provides a method to linearize the p/z-G_p plot and thereby predict the true original gas in place. A method is suggested to determine initial gas in place by analyzing the behavior of cumulative effective compressibility backcalculated from pressure-production data. The $\bar{c}_e(p)$ function determined by this procedure, or estimated from logs and geological maps (when sufficient production data is not available), is then used to forecast pressure-cumulative behavior.

For most reservoirs $\bar{c}_e$ is fairly constant through most of depletion. The magnitude of $\bar{c}_e(p)$ at initial pressure usually ranges from 15 to $100(10^{-6})$ psi^{-1}, depending mostly on the volume of water associated with the gas reservoir. As defined in this paper, all components of $\bar{c}_e$ represent cumulative volume changes; i.e., instantaneous water and rock compressibilities are *not* used directly.

We show that the effect of pore collapse on high pressure gas reservoirs is generally positive, providing additional pressure support. There is *not* a clear discontinuity in the behavior of p/z-G_p where pore collapse occurs, and pore collapse tends to flatten or increase p/z-G_p at lower pressures.

$\bar{c}_e$ may increase significantly at lower pressures because of gas solubility effects. An example is given for a large gas reservoir with high-CO_2 content that requires an increasing $\bar{c}_e$ term at lower pressures to linearize the p/z-G_p plot; the increasing $\bar{c}_e$ behavior is substantiated by calculations based on gas solubility effects.

The proposed gas material balance is applicable (and should be applied) to any high pressure gas reservoir with an appreciable volume of associated water. Numerous field examples are provided showing the application of the material balance equation to high pressure gas reservoirs.

Introduction

High pressure gas reservoirs experiencing depletion drive typically have downward curving p/z-G_p behavior. Incorrect extrapolation of early depletion data may result in serious over estimation of original gas in place and remaining reserves. Bruns et al.[1] work in 1965 was a result of a field study conducted on a large moderately overpressured gas reservoir in the Texas Gulf Coast area. Investments were made, and never needed, based on linear extrapolation of the early field p/z-G_p performance to an apparent original gas in place that was later found to be overstated by about 200 Bscf. Fig. 5 in Ref. 1 (Run 20) shows the concave downward curvature typical for the pressure response of a conventional limited external aquifer system that simulated the reservoir's response.

This type of "limited" aquifer behavior where pressure in the reservoir and aquifer are virtually equal led to the derivation in 1969 of a general material balance for high pressure gas reservoirs. The derivation includes pressure-dependent rock and water compressibility (with gas evolving from solution). All water and rock volumes associated with the reservoir and available for expansion, including a limited aquifer volume, were included in a cumulative effective compressibility term $\bar{c}_e(p)$. Rock and water compressibilities were defined to account for cumulative changes in pore volume to be multiplied by the cumulative pressure drop (p_i-p); instantaneous compressibilities are not used at all. The final form of the material balance is similar to that published by Ramogast and Farshad[2], except

References and illustrations at end of paper.

that Ref. 2 considered $\bar{c}_e$ as a constant. The 1969 derivation as presented in this paper defines a cumulative effective compressibility $\bar{c}_e(p)$ as a function of pressure expressed in terms of reservoir properties and volumes.

Literature Review

Harville and Hawkins[3] and Hammerlindl[4] attribute the concave downward shape of p/z-G_p curves obtained in abnormally pressured gas reservoirs entirely to pore collapse and formation compaction. No definition of pore collapse is given in Ref. 3, but a plot of backcalculated pore volume change indicated a system compressibility change from $28(10^{-6})$ psi^{-1} at initial pressure to about $6(10^{-6})$ psi^{-1} at low pressures. This magnitude of pore volume change implies associated water volume. The decreasing "system" compressibility is expected for an overpressured reservoir with pressure dependent pore volume compressibility, and based on results presented in this paper pore collapse is *not* a necessary condition for such behavior.

The Anderson "L" reservoir performance presented by Duggan[5] shows curved p/z-G_p field behavior which was primarily attributed to shale water influx with no evidence of reservoir pore compaction. The water influx drive mechanism was supported by the fact that several wells watered out. Wallace[6], in a 1969 paper, also concluded that shale water influx is an important drive mechanism in abnormally pressured gas reservoirs. Bass[7] discounts shale water influx, and attributes curved p/z-G_p behavior to peripheral water influx from a limited aquifer and formation compaction treated with a constant pore volume compressibility c_f. For a limited aquifer Bass defines a term F_p as the ratio of peripheral water pore volume to the pore volume of gas-bearing rock.

Roach[8] and Ramagost and Farshad[2] both utilize the term p/z[1-$c_e(p_i-p)$] for geopressured and abnormally pressured gas reservoirs. Both authors consider c_e a constant and they consider only the Anderson "L" example.

Bernard[9] does not accept the rock collapse theory as the cause for overpressured p/z-G_p behavior, concluding that water influx is the basic drive mechanism. He also uses p/z[1-c(p_i-p)] where c is a "catch-all" approximation for treating the effects of rock and water compressibility, a small steady-state acting aquifer, and steady state shale water influx. He further states that the term c is virtually impossible to quantify in terms of reservoir properties.

Begland and Whitehead[10], Prasad and Rogers[11], and Wang and Teasdale[12] all present studies of overpressured gas reservoirs based on computer models. Refs. 10 and 11 treat c_f and c_w as functions of pressure, including the effect of solution gas in the water. External water sources are also included in Refs. 11 and 12. The differential forms of the material balance used in these references correctly apply instantaneous compressibility in a history matching approach to determine initial gas in place. A direct plot of (p/z)[1-$\bar{c}_e(p_i-p)$] versus G_p was not made because the $\bar{c}_e$ term had not been defined.

Poston and Chen[13] analyzed several abnormally pressured gas reservoirs, and recognized that calculated values of $c_e > 30(10^{-6})$ psi^{-1} required to linearize the material balance equation reflected the influence of water influx.

Bourgoyne[14] demonstrates that reasonable values of shale permeability and compressibilities treated as a function of pressure can be used to match abnormal gas reservoir performance behavior. He points out, however, that determining k and c_f of the shale necessary for modelling this behavior is virtually impossible.

Ambastha[15] uses Bourgoyne's general material balance equation to develop a graphical matching technique based on a constant effective compressibility c_e. The example considered shows a lack of uniqueness in determining initial gas in place.

General Material Balance

The general form of the gas material balance derived in Appendix A is:

$$\frac{p}{z}\left[1-\bar{c}_e(p)(p_i-p)\right] = (p/z)_i - \frac{(p/z)_i}{G}\left[G_p - G_{inj} + W_pR_{sw} + \frac{5.615}{B_g}\left(W_pB_w - W_{inj}B_w - W_e\right)\right] \quad (2)$$

which reduces to Eq. 1 when water terms and gas injection can be neglected. The cumulative effective compressibility term $\bar{c}_e(p)$ is pressure dependent consisting of a cumulative pore volume compressibility $\bar{c}_f(p)$, cumulative total water compressibility $\bar{c}_{tw}(p)$, and the total pore and water volumes associated (i.e. in pressure communication) with the gas reservoir,

$$\bar{c}_e(p) = \frac{S_{wi}\bar{c}_{tw}(p)+\bar{c}_f(p)+M[\bar{c}_{tw}(p)+\bar{c}_f(p)]}{1-S_{wi}} \quad \ldots\ldots\ldots\ldots (3)$$

The formation and total water compressibility terms $\bar{c}_f$ and $\bar{c}_{tw}$ account for cumulative changes in pore volume from initial pressure to the current pressure.

The interbedded non-pay volume and limited aquifer contributions to pressure support are quantified in terms of the M ratio,

$$M = \frac{V_{pNNP}\,(\text{NON-NET PAY}) + V_{pAQ}\,(\text{LIMITED AQUIFER})}{V_{pR}\,(\text{NET PAY RESERVOIR})} \quad (4)$$

An important aspect of the material balance for high-pressure gas reservoirs is that the gas in solution in the connate and associated water provide both pressure support and additional gas available for production. The level of pressure support provided by the evolved solution gas depends on the level of depletion, and it is shown that this support is significant below about 1500 psia. The solution gas available for production also depends on the level of depletion, i.e. how much of the original solution gas has evolved [$R_{sw}(p_i)$-$R_{sw}(p)$] and the quantity of this gas that is mobile.

The term G is used for the *initial free gas in place*, and it is this quantity that will be determined from the material balance plot given by Eq. 1 when extrapolated to (p/z)[1-$\bar{c}_e(p_i-p)$]=0. This condition is reached at a pressure when $\bar{c}_e(p)(p_i-p)=0$, and not when p=0, i.e. additional gas may be produced after G_p reaches original free gas in place G. At pressures where G_p exceeds G the corrected p/z term (p/z)[1-$\bar{c}_e(p_i-p)$] becomes negative. If pressure could be brought to standard conditions ($p=p_{sc}$) the total gas produced would be G plus the total solution gas in place G_s, $G_p(@p_{sc})=G+G_s$.

The effect of connate water saturation S_{wi} and M are important to the magnitude of $\bar{c}_e$. With typical values of $\bar{c}_f=c_f=4(10^{-6})$ psi^{-1} and $\bar{c}_{tw}=c_{wi}=3(10^{-6})$ psi^{-1} for a high-pressured Gulf Coast sandstone reservoir the cumulative effective compressibility is initially $\bar{c}_e=7.5(10^{-6})$ psi^{-1} for $S_{wi}=35\%$ and M=0; and $\bar{c}_e=15(10^{-6})$ for $S_{wi}=35\%$ and M=1. Fig. 1 shows the percentage of true original free gas in place that would be overestimated by extrapolating early p/z-G_p data, indicating that the overestimation is greater for larger initial pressure and higher $\bar{c}_e$ values at initial conditions. For an initial pressure of 10,000 psia and a $\bar{c}_e=10(10^{-6})$ psi^{-1} the extrapolation of early data gives an estimate of G that is about 25 percent higher than the true original free gas in place. The sections below discuss the calculation of $\bar{c}_f(p)$ and $\bar{c}_{tw}(p)$ functions.

Cumulative Pore Volume Compressibility $\bar{c}_f$. The material balance presented in this paper uses a *cumulative* pore volume compressibility $\bar{c}_f$ defined as

$$\bar{c}_f(p) = \frac{1}{V_{pi}}\left[\frac{V_{pi}-V_p(p)}{p_i-p}\right] \quad \ldots\ldots\ldots\ldots\ldots\ldots (5)$$

The term in brackets is the slope of the chord from the initial condition (p_i, V_{p_i}) to any lower pressure (p, V_p), as shown in Fig. 2. This implies that $\bar{c}_f$ is a function of both pressure and the initial condition. The instantaneous pore volume compressibility c_f is defined as

$$c_f(p) = \frac{1}{V_p}\frac{\partial V_p}{\partial p} \quad \ldots\ldots\ldots\ldots\ldots\ldots\ldots\ldots\ldots\ldots (6)$$

and is *only* a function of pressure. At initial pressure the two pore volume compressibilities are equal: $\bar{c}_f(p_i) = c_f(p_i)$. The instantaneous compressibility function $c_f(p)$ should be used in reservoir simulation and differential forms of the material balance, while the cumulative compressibility function $\bar{c}_f(p)$ should be used with forms of the material balance that apply the cumulative pressure drop $(p_i - p)$, i.e. p/z vs G_p plots.

The pressure dependence of $\bar{c}_f$ is best determined by special core analysis under appropriate reservoir conditions. Table 1 summarizes the calculation of $\bar{c}_f$ as a function of pressure using laboratory data for a Gulf Coast sandstone. Fig. 3 shows how c_f and $\bar{c}_f$ vary as a function of pressure for this overpressured reservoir rock.

In the absence of pore collapse $\bar{c}_f$ is always greater than or equal to c_f. The cumulative pore volume compressibility remains higher than the instantaneous compressibility because of an averaging effect that reduces the pressure dependence of $\bar{c}_f$ compared with c_f. An important consequence of this behavior is that a rock exhibiting large pore volume change because of a high level of overpressure (and consequently with a high initial c_f value dropping rapidly to a "normal" value) will initially have and maintain a high cumulative compressibility $\bar{c}_f$ as shown in Fig. 3.

Pore collapse is defined as the condition when a rock's instantaneous pore volume compressibility starts to increase at decreasing reservoir pressure. Pore collapse provides greater pressure support when collapse occurs at a high pressure. However, pore collapse is not reflected by the $\bar{c}_f(p)$ function and will not therefore be seen on the p/z-G_p plot at the pressure when pore collapse occurs. In fact pore collapse may not be identifiable at all on the cumulative compressibility term. For example, the Gulf Coast sandstone in Fig. 3 exhibits pore collapse at 4000 psia (about 5000 psi less than initial pressure p_i). Despite the increase in c_f from 4 to $25(10^{-6})$ psi^{-1} in the pressure range 4000 to 1000 psia, the change in $\bar{c}_f$ over the same pressure range is almost insignificant. Fig. 4 shows a North Sea Chalk sample from a reservoir with initial pressure of 7000 psia exhibiting pore collapse at 6000 psia. Here the effect of pore collapse is greater, causing $\bar{c}_f$ to increase from 6 to $20(10^{-6})$ psi^{-1} in the pressure range from 6000 to 2000 psia. *In general, however, pore collapse in and of itself does not have a significant effect on the p/z-G_p plot.*

In the absence of laboratory data, pore volume compressibilities can be estimated from correlations presented by Hall[16] and by Von Gonten and Choudhary[17]. Hall's correlation (his Fig. 2) gives instantaneous pore volume compressibility as a function of porosity, i.e. there is no pressure dependence. The Hall correlation is probably adequate for normal pressured reservoirs. Von Gonten develops correlations for instantaneous pore volume compressibility c_f as a function of net overburden pressure (p_o), where p_o equals the overburden gradient times depth minus reservoir pressure.

Table 2 gives example values of initial pore volume compressibility $c_f(p_i)$ for overpressured and normal pressured reservoir conditions. Typically there are not large differences in c_f values for these two conditions.

Cumulative Total Water Compressibility $\bar{c}_{tw}$. The pressure support provided by water is made up of two components. First the water expansion with decreasing pressure, and second the release of solution gas and its expansion. The total or composite compressibility effect is expressed as

$$\bar{c}_{tw}(p) = \frac{1}{B_{tw}(p_i)}\frac{B_{tw}(p) - B_{tw}(p_i)}{p_i - p} \quad \ldots\ldots\ldots\ldots\ldots\ldots (7)$$

in terms of the total water formation volume factor B_{tw},

$$B_{tw}(p) = B_w(p) + \frac{[R_{swi} - R_{sw}(p)]B_g(p)}{5.615} \quad \ldots\ldots\ldots\ldots\ldots (8)$$

Fig. 5 shows typical behavior for B_w and B_{tw} as a function of pressure; the figure also shows the behavior of $\bar{c}_{tw}(p)$ where it is seen that little increase occurs before a pressure of about 1500 psia, and that at pressures below 1000 psia there is a significant increase in $\bar{c}_{tw}$ with a limiting relationship $\bar{c}_{tw} \propto 1/p$ at low pressures,

$$\bar{c}_{tw}(p \to 0) = \left[\frac{1}{5.615}\frac{Tp_{sc}}{T_{sc}}\frac{R_{swi}}{p_i B_{swi}}\right]\frac{1}{p} \quad \ldots\ldots\ldots\ldots\ldots (9)$$

Specifically at standard conditions (p_{sc}), $\bar{c}_{tw}$ is given by

$$\bar{c}_{tw}(p_{sc}) = \left[\frac{1}{5.615}\frac{T}{T_{sc}}\frac{R_{swi}}{p_i B_{wi}} - \frac{1}{p_i}\right] \quad \ldots\ldots\ldots\ldots\ldots (10)$$

To calculate $\bar{c}_{tw}$, values of B_w, R_{sw}, and B_g are tabulated with pressure as shown in Table 3. These properties can be obtained from correlations at pressures less than about 10,000 psia and 300°F. At more extreme conditions of pressure and temperature, and for gases with high concentrations of nonhydrocarbons CO_2, N_2, and H_2S, we have used the Peng-Robinson[18] equation of state with volume translation, and using binary interaction coefficients that are dependent on both temperature and salinity[19].

Another approach for high pressures is simply to extrapolate B_w linearly and R_{sw} with a flattening curvature towards a constant value. Nonhydrocarbons can be treated by evaluating R_{sw} of each component separately at its partial pressure, and summing the values for all soluble components

$$[R_{sw}(p)]_{TOTAL} = \sum_j [R_{sw}(y_j p)]_j \quad \ldots\ldots\ldots\ldots\ldots\ldots (11)$$

y_j is the reservoir gas mole fraction of component j. Typically the only components with appreciable solubility are methane, CO_2, and H_2S.

Associated Water Volume Ratio M. The total compressibility effect on the gas material balance depends on the magnitudes of rock and total water compressibilities *and* on the total pore and water volumes in pressure communication with the gas reservoir (including connate water and the pore volume within the net pay).

Associated water and pore volumes external to the net pay include non-net pay (NNP) such as interbedded shales and dirty sands, plus external water volume found in limited aquifers. Including these water volumes in reservoir simulation is referred to as using a "gross" model. In the proposed material balance equations this associated volume is expressed as a ratio relative to the pore volume of the net-pay reservoir,

$$M = M_{NNP} + M_{AQ} \quad \ldots\ldots\ldots\ldots\ldots\ldots\ldots\ldots (12)$$

where

$$M_{NNP} = \frac{V_{pNNP}\,(\text{INTERBEDDED NONNET PAY})}{V_{pR}\,(\text{NET PAY})} \quad \ldots\ldots (13)$$

$$M_{AQ} = \frac{V_{pAQ}\,(\text{AQUIFER})}{V_{pR}\,(\text{NET PAY})} \quad \ldots\ldots\ldots\ldots\ldots\ldots\ldots \quad (14)$$

In the simplest case when $M=0$ there will be pressure support only from connate water and the net-pay pore volume. This is equivalent in simulation to building a net model. The cumulative effective compressibility term $\bar{c}_e$ will then be expected to have values ranging from 7 to $15(10^{-6})$ psi^{-1} for normal-pressure reservoirs, where the larger values will generally result from high connate water saturation. Even larger values can be obtained in some overpressured reservoirs (see Table 2).

Net-pay compressibility effects alone can cause noticeable curvature in the p/z-G_p plot with potential overestimation of initial free gas in place (G) (see Fig. 1).

M_{NNP}. The non-net pay water volume ratio M_{NNP} is comprised of interbedded reservoir pore volume, including shales and poor quality rock, that are assumed to be completely filled with water. With this definition M_{NNP} can be written in terms of the net-to-gross ratio NGR defined as

$$NGR = \frac{h_R}{h_R+h_{NNP}} = \frac{h_R}{h_{GROSS}} \quad \ldots\ldots\ldots\ldots\ldots\ldots\ldots \quad (15)$$

Accounting for different porosities in the net pay and non-net pay M_{NNP} is given by

$$M_{NNP} = \frac{(\phi h A)_{NNP}}{(\phi h A)_R} = \frac{\phi_{NNP}}{\phi_R}\left[\frac{1-NGR}{NGR}\right] \quad \ldots\ldots\ldots\ldots\ldots\ldots \quad (16)$$

Properties and thicknesses of the net pay and non-net pay are readily available from log analysis.

If the non-net pay pore volume is known to have an initial gas saturation, albeit immobile, the material balance is readily modified to account for this fact; the term $M_{NNP}(\bar{c}_f+\bar{c}_{tw})$ is replaced by $M_{NNP}[\bar{c}_f+S_{wi,NNP}\bar{c}_{tw}]$ and the initial gas volume is included in the total original free gas in place G.

M_{AQ}. Aquifers with sufficient permeability and limited areal extent can be treated as part of the total cumulative compressibility term. The water volume ratio of the aquifer M_{AQ} can be determined using geological maps and well control to define areal extent, and electric logs to define the gas-water contact. In general, M_{AQ} is defined as

$$M_{AQ} = \frac{(\phi h A)_{AQ}}{(\phi h A)_R} \quad \ldots\ldots\ldots\ldots\ldots\ldots\ldots\ldots \quad (17)$$

and for a radial aquifer geometry quantified in terms of the aquifer-to-reservoir radius r_{AQ}/r_R, the aquifer volume ratio can be expressed

$$M_{AQ} = \frac{(\phi h)_{AQ}}{(\phi h)_R}\left[(r_{AQ}/r_R)^2 - 1\right] \quad \ldots\ldots\ldots\ldots\ldots\ldots \quad (18)$$

Bruns et al.[1] show that limited aquifers with r_{AQ}/r_R ratios up to 5 have the same p/z-G_p behavior for permeabilities 100 md and higher. This implies that the transient effects in the aquifer have negligible effect on reservoir performance and the aquifer can be treated as part of the cumulative effective compressibility term. Values of M_{AQ} used in the definition of $\bar{c}_e$ may be as high as 25 [$M_{AQ}=(r_{AQ}/r_R)^2-1$] in reservoirs with moderate permeability. With higher permeabilities limited aquifers can include r_{AQ}/r_R ratios greater than 5 and still be treated as part of the cumulative effective compressibility term.

When the aquifer is sufficiently large and requires treatment with either superposition or the Schilthius infinite aquifer model, the $\bar{c}_e$ term should still be used but it will only contain the effect of net pay and non-net pay volumes, i.e. $M=M_{NNP}$.

Cumulative Effective Compressibility $\bar{c}_e$. Total cumulative effective compressibility represents *all* available pressure support from rock and water. The equation for $\bar{c}_e$ is

$$\bar{c}_e(p) = \frac{S_{wi}\bar{c}_{tw}(p)+\bar{c}_f(p)+M[\bar{c}_{tw}(p)+\bar{c}_f(p)]}{1-S_{wi}} \quad \ldots\ldots\ldots\ldots \quad (19)$$

For a specific reservoir a family of $\bar{c}_e(p)$ curves can be generated for several M values. These curves will have specific characteristics depending on the pressure dependence of rock and water compressibilities. The $\bar{c}_{tw}(p)$ curves are relatively constant at high pressure, increasing slightly as pressure decreases, then rising sharply at low pressure around 1000 psia. Typically a constant pore volume compressibility c_f can be assumed and the $\bar{c}_e(p)$ curves will then have the same character as the $\bar{c}_{tw}(p)$ curve. Fig. 6 illustrates an example of $\bar{c}_e(p)$ curves at various M ratios for a typical Gulf Coast reservoir with $p_i=9000$ psia, $T=200°F$, $\gamma_g=0.7$ (air=1), and a constant $\bar{c}_f=3.2(10^{-6})$ psi^{-1}.

For overpressured reservoirs exhibiting a pressure-dependent $\bar{c}_f(p)$, the family of $\bar{c}_e(p)$ curves *at high pressures* will tend to decrease with depletion. In the absence of pore collapse $\bar{c}_f(p)$ decreases to a constant value at lower pressure and the $\bar{c}_e(p)$ curves at lower pressure are dominated by the increasing $\bar{c}_{tw}(p)$ function. If pore collapse occurs, but not early in depletion, the pore collapse is almost insignificant because (a) the $\bar{c}_f(p)$ function does not start increasing until low pressures because it represents a cumulative pore volume change, and (b) when the $\bar{c}_f(p)$ function finally starts to increase it will be masked by the $\bar{c}_{tw}(p)$ function which is increasing as 1/p. Fig. 7 illustrates this point for a Gulf Coast overpressured reservoir with $p_i=9000$ psia, $T=300°F$, and $\gamma_g=0.71$ (air=1). Although pore collapse occurs at 4000 psia (Fig. 3), $\bar{c}_f$ does not start increasing until 2000 psia. The increase is insignificant relative to the increase in $\bar{c}_{tw}(p)$ at lower pressures.

The next example is a North Sea chalk (Fig. 4) that shows pore collapse at a pressure only 1000 psi below initial pressure of 7000 psia. The $\bar{c}_f(p)$ function increases almost simultaneously with instantaneous c_f, and the effect of $\bar{c}_f(p)$ on $\bar{c}_e(p)$ is shown in Fig. 8. Although $\bar{c}_f(p)$ has an impact on $\bar{c}_e(p)$ at moderate and high pressures for this example, the $\bar{c}_{tw}(p)$ function still dominates the behavior of $\bar{c}_e(p)$ at pressures less than 1500 psia.

Estimating Gas-In-Place. A method is proposed for estimating the initial (free) gas in place G based on historical pressure-cumulative data. The procedure also determines the water volume ratio M and the $\bar{c}_e(p)$ function. First, a plot of p/z versus cumulative gas production G_p should have the characteristic concave downward shape of a high-pressure reservoir influenced by associated water and pore volume compressibility.

A range of values for G should then be assumed, with the largest value based on an extrapolation of the early depletion data and the lowest value being somewhat larger than the current G_p. For an assumed value of G, calculate for each measured p/z and G_p data the $\bar{c}_e$ value from the rearranged material balance equation (Eq. 1),

$$(\bar{c}_e)_{BACKCALCULATED} = \left[1-\frac{(p/z)_i}{(p/z)}\left(1-\frac{G_p}{G}\right)\right]\frac{1}{(p_i-p)} \quad \ldots\ldots \quad (20)$$

At this point, a plot can be made of backcalculated $\bar{c}_e$ as a function of pressure given the assumed G. Using reservoir rock and water properties, a family of $\bar{c}_e(p)$ curves at various M values can be generated to match against the backcalculated $\bar{c}_e$ values. The data should

honor the shape and magnitude of one $\bar{c}_e(p)$ curve, where this match yields G, the M value, and a $\bar{c}_e(p)$ function that can be used to forecast future p/z-G_p behavior. This procedure gives a sound physical significance to the estimation of G as opposed to a pure statistical best-fit that may lead to unrealistic solutions. The Field Examples section discusses criteria for matching field data, and the expected behavior of $\bar{c}_e(p)$.

Characteristics of p/z-G_p Plots for High-Pressure Reservoirs

Pore volume reduction, water expansion, and solution gas evolution, expressed in terms of $\bar{c}_e(p)$ in the general material balance equation, provide pressure support for *all* reservoirs during depletion. The reservoir does not have to be overpressured or geopressured. The term $\bar{c}_e(p)(p_i-p)$ determines whether the conventional p/z-G_p plot yields a straight line. For most low-pressure reservoirs this term is small and is often neglected because a straight-line p/z-G_p plot is obtained. Reservoirs undergoing depletion with initial pressure exceeding 5000 psia are automatically candidates for being treated with the complete material balance equation.

Fig. 9 presents three generated p/z-G_p curves for a Gulf Coast overpressured sandstone reservoir using M=0 (i.e. $\bar{c}_e(p)=[\bar{c}_f(p)+S_{wi}\bar{c}_{tw}(p)]/(1-S_{wi})$. Curve A accounts for pore volume reduction including pore collapse at about 4000 psia. Curve B uses the same $\bar{c}_f(p)$ function as Curve A down to 4000 psia (where pore collapse occurs) and thereafter uses a constant instantaneous compressibility of $4(10^{-6})$ psi^{-1}. p/z-G_p plots for A and B are almost identical, showing only a slight separation at pressures less than 3500 psia. This clearly shows the limited effect of pore collapse on the p/z-G_p plot when collapse occurs late in depletion. Curve C assumes, *unrealistically*, that the initial pore volume compressibility of $13(10^{-6})$ psi^{-1} remains constant throughout depletion. The difference between the two p/z-G_p curves A and C is a result of the actual decrease in pore volume compressibility. Including an external water volume quantified with M=2 produces more curvature in the p/z-G_p plots, but the separation between curves with and without pore collapse is still very small (not shown).

Another example relates to a North Sea chalk reservoir where pore collapse occurs just below initial pressure. Fig. 10 presents generated p/z-G_p plots for M=0 with pore collapse (curve A) and with no pore collapse (curve B). The effect of pore collapse is more significant than in the previous example because it occurs at a relatively high pressure.

Field Examples

Ellenburger Gas Reservoir. This field example is for a normal pressured (0.5 psi/ft) 1600-foot thick, dry gas reservoir with initial reservoir pressure of 6675 psia at 200°F. Average porosity is about 5.0% with connate water saturation in the pay of about 35%. Permeability is high because of an extensive microfracture system that results in a high degree of interwell pressure communication and almost instantaneous pressure buildup to static conditions. Initial CO_2 concentration was about 28 mol-%, and a gradual increase in CO_2 concentration to 31 mol-% has been observed. The reservoir has produced about 3.1 Tscf and currently has an average fieldwide bottomhole pressure of approximately 1000 psia. The p/z-G_p plot shows a characteristic concave downward behavior, with an initial gas in place estimate of more than 4.4 Tscf using early data (Fig. 11). The p/z-G_p data at low pressures has started flattening.

The procedure outlined earlier for determining initial free gas in place G was used for this reservoir. Fig. 12 shows a plot of backcalculated $\bar{c}_e$ versus pressure for a range of G from 3.0 Tscf to 3.6 Tscf. Another plot of $\bar{c}_e(p)$ was generated for several values of M using $S_{wi}=0.35$, $\bar{c}_f=6.5(10^{-6})$ psi^{-1} (from Hall[16]), and $\bar{c}_{tw}(p)$ calculated from equation of state results. Fig. 13 shows the best-fit of data on the $\bar{c}_e(p)$ curve for M=3.3, corresponding to an initial free gas in place G=3.15 Tscf.

The total water volume including connate and associated waters is given by

$$W = \frac{1}{5.615}\frac{GB_{gi}}{B_{wi}}\frac{(S_{wi}+M)}{(1-S_{wi})} \quad \ldots\ldots\ldots\ldots\ldots\ldots\ldots (21)$$

which yields $8.45(10^9)$ STB. The initial solution gas in place G_s is equal to W times the initial solution gas-water ratio R_{swi},

$$G_s = W R_{swi} \quad \ldots\ldots\ldots\ldots\ldots\ldots\ldots\ldots\ldots\ldots (22)$$

Because of the high CO_2 concentration in this reservoir the solution gas-water ratio ($R_{swi}=67.5$ scf/STB) is about three times larger than for hydrocarbon gas systems. This yields a solution gas in place of $G_s=0.55$ Tscf and a total initial gas in place of $G+G_s=3.70$ Tscf. Fig 11 shows the p/z-G_p forecast using the M value determined from the match to calculate the $\bar{c}_e(p)$ function from S_{wi}, M, $\bar{c}_f$, and $\bar{c}_{tw}(p)$. Also shown on this figure is the plot of $(p/z)[1-\bar{c}_e(p)(p_i-p)]$ versus G_p for historical performance data and for the forecast, where it is seen that the current cumulative gas produced equals the original free gas in place.

The associated water volume given by M=3.3 consists of non-net pay and an external limited aquifer. Log analysis indicates a net-to-gross ratio NGR=0.5, $\phi_R=0.05$, and $\phi_{NNP}=0.03$, yielding $M_{NNP}=0.6$. External water is known to exist but has not been mapped due to lack of well control. The calculated aquifer water volume ratio $M_{AQ}=2.7$ (3.3-0.6), or an equivalent $r_{AQ}/r_R=1.9$, seems reasonable for a limited aquifer.

Anderson "L". This reservoir has been studied by several authors and it is perhaps the best recognized example of a high-pressure gas reservoir with concave downward p/z-G_p behavior (Fig. 14). The reservoir was abandoned after producing 55 Bscf, but pressure tests of public record were discontinued after 40 Bscf had been produced.

Different analyses by other authors have indicated original free gas in place between 65 to 75 Bscf. Fig. 15 shows backcalculated $\bar{c}_e$ versus pressure for values of G equal to 65, 72, and 90 Bscf. The 72 Bscf volume is chosen based on a best-fit match with the $\bar{c}_e(p)$ function calculated using M=2.25, $S_{wi}=0.35$, $\bar{c}_f=3.2(10^{-6})$ psi^{-1}, and a $\bar{c}_{tw}(p)$ function from equation of state results. Although the first four data do not fall on the slightly-increasing $\bar{c}_e(p)$ curve, data at pressures below this value do follow the trend down to the last pressure data near 3000 psia.

The 90 Bscf estimate produces unrealistically low $\bar{c}_e$ values, lower than would be calculated using the net reservoir pore volume and connate water compressibilities. The lowest estimate of 65 Bscf gives a shape for $\bar{c}_e(p)$ that cannot be accounted for using normal $\bar{c}_f(p)$ and $\bar{c}_{tw}(p)$ functions.

The forecasted p/z-G_p performance (Fig. 14) is calculated using the match determined above. Total gas in place of 76 Bscf which includes 72 Bscf of original free gas plus 4 Bscf of solution gas.

Cajun Field. This reservoir was originally reported by Stelly and Farshad[20] and recently analyzed by Ambastha[15]. Initial pressure is 11450 psia at 13,300 ft (0.86 psi/ft). Connate water saturation is reported as 22%. Production data is reported to a pressure of 6850 psia and a cumulative of 145 Bscf.

Using the p/z-G_p data shown in Fig. 16, backcalculated values of $\bar{c}_e$ are shown in Fig. 17. The range of values for G are the same as considered by Ambastha: 410 to 760 Bscf. The 760 Bscf estimate yields unacceptably low $\bar{c}_e$ values, less than $2(10^{-6})$ psi^{-1}. Values lower than 565 Bscf produce $\bar{c}_e(p)$ functions that increase more steeply than would be expected from $\bar{c}_{tw}(p)$ behavior. The expected magnitude and shape of cumulative effective compressibility is exhibited by the backcalculated $\bar{c}_e$ values for an assumed G of 650 Bscf. This

corresponds to M=0.2 using S_{wi}=0.22, $\bar{c}_f$=4(10^{-6}) psi^{-1}, and $\bar{c}_{nw}$(p) from correlations.

Gulf Coast Reservoir C. This example is taken from Bernard[9] (his Fig. 1) and represents a high-pressure, overpressured gas reservoir taken to a low abandonment pressure. The p/z-G_p plot (Fig. 18) shows significant concave downward character with an extrapolation of early data giving an initial free gas in place of 380 Bscf. Depletion from p_i=11500 psia to about 1200 psia produced 180 Bscf, verifying that the early-data extrapolation of 380 Bscf was incorrect.

Fig. 19 shows backcalculated $\bar{c}_e$(p) for values of G from 160 to 240 Bscf. The only curve that produces an approximately constant $\bar{c}_e$ at high pressures is G=160 Bscf, a value 30 Bscf less than the volume already produced. The curve for G=240 Bscf has a downward sloping $\bar{c}_e$(p) that becomes negative, also an unrealistic solution. The G=200 Bscf curve has a downward sloping $\bar{c}_e$(p) function that can be explained by a pressure-dependent pore volume compressibility. A highly overpressured formation can readily have a pressure-dependent $\bar{c}_f$(p) function, i.e. one that decreases with depletion.

Reservoir data was not presented by Bernard[9] for this field example, but making some assumptions about typical Gulf Coast reservoir properties we matched the $\bar{c}_e$(p) backcalculated behavior using G=185 Bscf, and a $\bar{c}_f$(p) function that decreased linearly by a factor of about 2 from initial conditions to abandonment pressure. The backcalculated $\bar{c}_e$(p) behavior at 2000 psia started increasing, indicating that pore collapse could have occurred earlier in depletion.

Duck Lake Field. Cason[21] presents production performance data from the Discorbis 1 reservoir in the Duck Lake field of southern Louisiana. This high-pressure gas reservoir was waterflooded for more than 10 years after first being depleted to about 1000 psia. Fig. 20 shows the p/z-cumulative plot for data prior to the waterflooding project, showing typical concave downward curvature.

Cason reports an initial gas in place of 680 Bscf using traditional water influx analysis. Based on the high reservoir permeability (k=1,750 md) we established that the reservoir performance could be analyzed with the general material balance where the external aquifer was treated as part of the $\bar{c}_e$ term. Using G=680 Bscf, $\bar{c}_e$(p) was backcalculated from the general material balance as shown in Fig. 21. The $\bar{c}_e$(p) behavior is flat throughout depletion. This behavior should be compared with the dashed line representing the expected $\bar{c}_e$(p) behavior based on Eq. 3 using a constant $\bar{c}_f$=3.4(10^{-6}) psi^{-1}, M=4.8, and an appropriate $\bar{c}_{nw}$(p) function. The dashed curve has significant increase in $\bar{c}_e$(p) already at 2000 psia, and the more-or-less constant $\bar{c}_e$(p) behavior backcalculated from production data can not be readily explained. It is expected, however, that conventional water influx analysis which assumes constant water and pore volume compressibility will yield an estimate of initial gas in place that reflects a constant $\bar{c}_e$ when backcalculated from the general gas material balance.

Using a smaller estimate of G=625 Bscf yields backcalculated $\bar{c}_e$(p) behavior that is very similar to $\bar{c}_e$(p) calculated from Eq. 3 using a constant $\bar{c}_f$=3.4(10^{-6}) psi^{-1}, M=6.5, and $\bar{c}_{nw}$(p) function. Cumulative production at abandonment was about 650 Bscf, indicating that about 25 Bscf of the total produced gas came from solution. Based on G=625 Bscf, R_{swi}=20.6 scf/STB, S_{wi}=0.18, and M=6.5 the initial *solution* gas in place is G_s=65 Bscf.

Conclusions

1. A general form of the material balance equation for gas reservoirs has been presented. This equation has particular application to high-pressure reservoirs. A cumulative effective compressibility term $\bar{c}_e$(p) has been defined in terms of pressure-dependent pore volume and total water cumulative compressibilities, $\bar{c}_f$(p) and $\bar{c}_{nw}$(p), and the total volume of water associated with the net pay reservoir expressed as a ratio M.

2. The general material balance equation applies to *all* high-pressure reservoirs, both normal pressured and abnormally pressured (overpressured and geopressured).

3. The effect of a limited aquifer can be included as part of the M term for most depletion-type reservoirs. Using the water volume ratio M in the cumulative effective compressibility term, together with normal values of $\bar{c}_f$ and $\bar{c}_{nw}$, explains the "large" $\bar{c}_e$ values commonly reported for high-pressure gas reservoirs when linearizing the material balance equation. In fact, large values of $\bar{c}_e$ backcalculated from field performance data indicate that associated water influx is a dominant drive mechanism.

4. Only *cumulative* compressibilities ($\bar{c}_f$ and $\bar{c}_{nw}$) can be used in the general gas material balance equation because they are applied against the cumulative pressure drop (p_i-p) in p/z-G_p plots. A method is given for calculating cumulative total water and pore volume compressibility $\bar{c}_{nw}$(p) and $\bar{c}_f$(p).

5. A method is proposed for estimating the original free gas in place from production data. This method uses backcalculated cumulative effective compressibility $\bar{c}_e$ which is plotted versus pressure and compared with expected $\bar{c}_e$(p) behavior calculated from rock and water properties for a range of values of the associated water volume ratio M.

6. In lieu of laboratory data for pore volume compaction we recommend Hall's[16] correlation for normal-pressured reservoirs, and Von Gonten's[17] correlation for abnormally-pressured reservoirs.

7. Pore collapse in and of itself does not contribute significantly to pressure support in overpressured gas reservoirs. In fact, pore collapse has little effect unless it occurs early in depletion at a relatively high pressure. The effect of pore collapse, if present, is a positive effect and tends to flatten the p/z-G_p curve, *not bending the curve downward* as has been implied by others.

8. Gas found initially in solution in the connate and associated water is an important component of pressure support late in depletion (below 1500 psia) and may contribute additional producible volumes of gas. Typically the solution gas in place G_s represents 2 to 10 percent of the original free gas in place, the value depending primarily on total water volume $(M+S_{wi})/(1-S_{wi})$ and the initial solution gas-water ratio R_{swi}. Gas reservoirs with high CO_2 concentration (>20 mol-%) can have even higher solution gas in place, G_s.

Nomenclature

A	=	area, ft^2 [m^2]
B	=	formation volume factor, reservoir per standard volume
c	=	instantaneous compressibility, 1/psi [1/kPa]
$\bar{c}$	=	cumulative compressibility, 1/psi [1/kPa]
G	=	original free gas-in-place, Bscf [std m^3]
G_p	=	cumulative gas production, Bscf [std m^3]
G_s	=	initial solution gas in place, Bscf [std m^3]
G_x	=	early overestimate of G, Bscf [std m^3]
G_{inj}	=	cumulative gas injection, Bscf [std ^{3}]
h	=	thickness, ft [m]
M	=	volume ratio, dimensionless
NGR	=	net-to-gross ratio, dimensionless
p	=	reservoir pressure, psia [kPa]
p_i	=	initial reservoir pressure, psia [kPa]
p_o	=	net overburden pressure, psia [kPa]
r_R	=	radius of reservoir, ft [m]
r_{AQ}	=	radius of aquifer, ft [m]
R_{sw}	=	solution gas water ratio, SCF/STB [std m^3/m^3]
S_{wi}	=	initial water saturation, fraction
T	=	reservoir temperature, °R [K]

V	=	volume, ft³ [m³]
V_p	=	pore volume, cm³ and ft³ [m³]
V_b	=	bulk volume, cm³ [m³]
W	=	total water in place, bbl [m³]
W_e	=	cumulative water influx, bbl [m³]
W_{inj}	=	cumulative water injection, bbl [m³]
W_p	=	cumulative water production, bbl [m³]
z	=	gas compressibility factor, dimensionless
ϕ	=	porosity, fraction

Subscripts

A	=	associated water
AQ	=	limited aquifer
e	=	effective
f	=	pore volume ("formation")
g	=	gas
GROSS	=	gross interval thickness
i	=	initial
inj	=	injection
NNP	=	non-net pay
R	=	reservoir
sc	=	standard conditions
tw	=	total water
w	=	water

Acknowledgements

We thank the management of Phillips Petroleum Company for permission to publish this paper. We also acknowledge Fred Kent for work done on the Ellenburger example.

References

1. Bruns, J.R., Fetkovich, M.J., and Meitzen, V.C.: "The Effect of Water Influx on p/z-Cumulative Gas Production Curves," *JPT* (March 1965) 287-91.
2. Ramagost, B. P. and Farshad, F. F.: "p/z Abnormal Pressured Gas Reservoirs," paper 10125 presented at the 56th Annual Meeting of SPE of AIME, San Antonio, TX, (Oct. 5-7, 1981).
3. Harville, D. W. and Hawkins, M. F. Jr.: "Rock Compressibility and Failure as Reservoir Mechanisms in Geopressured Gas Reservoirs," *JPT* (Dec. 1969)1528-30.
4. Hammerlindl, D. J.: "Predicting Gas Reserves in Abnormally Pressured Reservoirs," paper SPE 3479 presented at the 46th Annual Meeting of SPE of AIME, New Orleans, LA, (Oct. 3-6, 1971).
5. Duggan, J. O.: "The Anderson "L" - An Abnormally Pressured Gas Reservoir in South Texas," *JPT* (Feb. 1971)132-138.
6. Wallace, W.E.: "Water Production from Abnormally Pressured Gas Reservoirs in Louisiana," *JPT* (Aug., 1968) 969-982.
7. Bass, D.M.: "Analysis of Abnormally Pressured Gas Reservoirs with Partial Water Influx," paper SPE 3850 presented at the 1972 Abnormal Subsurface Pressure Symposium, May 15-16.
8. Roach, R. H.: "Analyzing Geopressured Reservoirs - A Material Balance Technique," paper SPE 9968 (1981).
9. Bernard, W. J.: "Gulf Coast Geopressured Gas Reservoirs: Drive Mechanism and Performance Prediction," paper SPE 14362 presented at the 60th Annual Meeting of SPE of AIME, Las Vegas, NV, (Sept. 22-25, 1985).
10. Begland, T. F. and Whitehead, W. R.: "Depletion Performance of Volumetric High Pressured Gas Reservoirs," SPE Reservoir Engineering (Aug. 1989) 279-282. SPE 15523 first presented at the SPE Annual Meeting (Oct. 5-8, 1986) New Orleans, LA.
11. Prasad, R. K. and Rogers, L. A.: "Superpressured Gas Reservoirs: Case Studies and a Generalized Tank Model," paper SPE 16861 presented at the 62nd Annual Meeting of SPE of AIME, Dallas, TX, (Sept. 27-30, 1987).
12. Wang, B. and Teasdale, T.S.: "GASWAT-PC: A Microcomputer Program for Gas Material Balance With Water Influx," paper SPE 16484 presented at the 1987 Petroleum Industry Applications of Microcomputers held in Del Lago on Lake Conroe, Montgomery Texas, June 23-26, 1987.
13. Poston, S. W. and Chen, H. Y.: "Case History Studies: Abnormal Pressured Gas Reservoirs," paper SPE 18857.
14. Bourgoyne, A.T. Jr.: "Shale Water as a Pressure Support Mechanism in Gas Reservoirs Having Abnormal Formation Pressure," *J.Pet.Science*, 3(1990)305-319.
15. Ambastha, A. K.: "Analysis of Material Balance Equations for Gas Reservoirs," Paper No. CIM/SPE 90-36, June 10-13, 1990.
16. Hall, H.N.: "Compressibility of Reservoir Rocks," Trans AIME (1953)198,309-311.
17. Von Gonten, W. D. and Choudhary, B. K.: "The Effect of Pressure and Temperature on Pore-Volume Compressibility," paper SPE 2526 presented at the Annual Meeting of SPE of AIME, Denver, CO (Sept. 28-Oct. 1, 1969).
18. Peng, D.-Y. and Robinson, D.B.: "A New Two-Constant Equation of State," *Ind.Eng.Chem.Fund.*, No. 1 (1976) 59-64.
19. Soreide, I. and Whitson, C.H.: "Mutual Solubilities of Petroleum Reservoir Fluids Including Brine From a Cubic Equation of State," paper submitted for publication in *Fluid Phase Equilibria* (April 10, 1990).
20. Stelly, O.V. and Farshad, F.F.: "Predicting Gas In Place In Abnormal Reservoirs," *Pet.Eng.*(June 1981) 104-110.
21. Cason, L. D. Jr.: "Waterflooding Increases Gas Recovery," *J.Pet.Tech.* (Oct. 1989)1102-1106.

Appendix A _ Derivation of General Gas Material Balance

The derivation that follows is based on the following assumptions:

1. Any pressure change caused by production or injection into the reservoir will be felt immediately throughout the total system including:

a. *Net Pay Reservoir* ("R").

b. *Non-Net Pay* ("NNP") including interbedded shales and poor quality rock assumed to be 100% water saturated.

c. *Limited Aquifer* ("AQ"), when present, also assumed to be water saturated.

The non-net pay and aquifer volumes are referred to as "associated" water volumes and both contribute to water influx during depletion.

2. Simple modifications to the material balance equations can be made to generalize for non-net pay that has an initial free gas saturation.

3. All water in the system is initially saturated with solution gas.

Fig. 22 shows a schematic of the reservoir/associated water system.

Practically, the assumption of equal pressure throughout the system is reasonable, and any transients effects caused by a large aquifer may be treated by a conventional water influx term (W_e) as shown below.

For the sake of brevity we have chosen to omit explicit reference to pressure dependence - i.e. $\bar{c}_e$, $\bar{c}_f$, and $\bar{c}_{tw}$ should actually read $\bar{c}_e(p)$, $\bar{c}_f(p)$, and $\bar{c}_{tw}(p)$.

Derivation. The volumetric balance at any pressure states that the total pore volume ($V_{pR}+V_{pA}$) equals the net reservoir pore volume occupied by gas and water ($V_{gR}+V_{wR}$) plus the associated (non-net pay and aquifer) pore volume which also is occupied by gas and water ($V_{gA}+V_{wA}$):

$$(V_{pR}+V_{pA}) = (V_{gR}+V_{wR}) + (V_{gA}+V_{wA}) \quad \ldots\ldots\ldots\ldots (A1)$$

The net-pay reservoir pore volume V_{pR} is given by the initial volume V_{pRi} less the change in pore volume ΔV_{pR},

$$V_{pR} = V_{pRi}-\Delta V_{pR} \quad \ldots\ldots\ldots\ldots\ldots\ldots\ldots (A2)$$

$$V_{pRi} = V_{gRi} + V_{wRi}$$

$$V_{pRi} = GB_{gi} + \frac{GB_{gi}}{1-S_{wi}} S_{wi} \quad \ldots\ldots\ldots\ldots\ldots\ldots (A3)$$

$$\Delta V_{pR} = \frac{GB_{gi}}{1-S_{wi}} \bar{c}_f (p_i-p) \;\; ; \;\; \bar{c}_f = (\bar{c}_f)_R \quad \ldots\ldots\ldots\ldots (A4)$$

yielding

$$V_{pR} = GB_{gi} + \frac{GB_{gi}}{1-S_{wi}} S_{wi} - \frac{GB_{gi}}{1-S_{wi}} \bar{c}_f (p_i-p) \quad \ldots\ldots\ldots (A5)$$

Pore volume of the associated rock is given by the initial pore volume less the change in pore volume,

$$V_{pA} = V_{pAi} - \Delta V_{pA} \quad \ldots\ldots\ldots\ldots\ldots\ldots\ldots (A6)$$

$$V_{pAi} = \frac{GB_{gi}}{1-S_{wi}} M \quad \ldots\ldots\ldots\ldots\ldots\ldots\ldots (A7)$$

$$\Delta V_{pA} = \frac{GB_{gi}}{1-S_{wi}} M \bar{c}_f (p_i-p) \;\; ; \;\; \bar{c}_f = (\bar{c}_f)_A \quad \ldots\ldots\ldots\ldots (A8)$$

yielding

$$V_{pA} = \frac{GB_{gi}}{1-S_{wi}} M - \frac{GB_{gi}}{1-S_{wi}} M \bar{c}_f (p_i-p) \quad \ldots\ldots\ldots\ldots (A9)$$

The net reservoir gas volume is given by the sum of unproduced free gas, gas released from solution, and any injected gas,

$$V_{gR} = (V_{gR})_{\substack{\text{Unproduced}\\ \text{Free Gas}}} + (V_{gR})_{\substack{\text{Released}\\ \text{From Solution}}} + (V_{gR})_{\text{Injected}} \quad \ldots\ldots (A10)$$

$$(V_{gR})_{\substack{\text{Unproduced}\\ \text{Free Gas}}} = [G-(G_p-W_pR_{sw})]B_g \quad \ldots\ldots\ldots\ldots (A11)$$

$$(V_{gR})_{\substack{\text{Released}\\ \text{From Solution}}} = \frac{GB_{gi}}{1-S_{wi}} \frac{S_{wi}}{B_{wi}} (R_{swi}-R_{sw}) B_g \frac{1}{5.615} \quad \ldots\ldots (A12)$$

$$(V_{gR})_{\text{Injected}} = G_{inj} B_g \quad \ldots\ldots\ldots\ldots\ldots\ldots (A13)$$

resulting in

$$V_{gR} = [G-(G_p-W_pR_{sw})]B_g + \frac{GB_{gi}}{1-S_{wi}} \frac{S_{wi}}{B_{wi}} (R_{swi}-R_{sw}) \frac{B_g}{5.615} + G_{inj} B_g \quad \ldots\ldots\ldots\ldots (A14)$$

PVT properties B_g and R_{sw} are evaluated at current reservoir pressure. G_p for a gas condensate is the wet gas volume calculated by adding separator gas to liquid condensate converted to an equivalent surface gas volume. Also, the two-phase Z-factor must be used to calculated B_g for gas condensate reservoirs. Strictly speaking the cumulative water production term W_p represents "free" water production and not the water condensed out of solution from the produced gas wellstream.

The gas volume in the associated pore volume is a function of the amount of gas that has come out of solution,

$$V_{gA} = \frac{GB_{gi}}{1-S_{wi}} M \frac{1}{B_{wi}} (R_{swi}-R_{sw}) B_g \frac{1}{5.615} \quad \ldots\ldots\ldots\ldots (A15)$$

The water volume in the net-pay reservoir equals the unproduced initial water plus injected water plus water encroachment from an external aquifer,

$$V_{wR} = (V_{wR})_{\text{Unproduced}} + (V_{wR})_{\text{Injected}} + [(V^e_{wR})_{\text{Encroachment}}] \quad \ldots\ldots (A16)$$

$$(V_{wR})_{\text{Unproduced}} = \frac{GB_{gi}}{1-S_{wi}} \frac{S_{wi}}{B_{wi}} B_w - W_pB_w \frac{1}{5.615} \quad \ldots\ldots\ldots (A17)$$

$$(V_{wR})_{\text{Injected}} = 5.615\, W_{inj}\, B_w \quad \ldots\ldots\ldots\ldots\ldots\ldots (A18)$$

$$(V_{wR})_{\text{Encroachment}} = 5.615\, W_e \quad \ldots\ldots\ldots\ldots\ldots\ldots (A19)$$

yielding

$$V_{wR} = \frac{GB_{gi}}{1-S_{wi}} \frac{S_{wi}}{B_{wi}} B_w + 5.615(W_{inj}B_w+W_e-W_pB_w) \quad \ldots\ldots (A20)$$

The aquifer encroachment term W_e represents any external water volume that is not already included in the "M" term. Later in the derivation we show the conditions required so that water encroachment (treated rigorously by the method of superposition) can be included as part of the M term used in the cumulative effective compressibility $\bar{c}_e$.

The water volume in the associated pore volume is given by simple expansion,

$$V_{wA} = \frac{GB_{gi}}{1-S_{wi}} M \frac{1}{B_{wi}} B_w \quad \ldots\ldots\ldots\ldots\ldots\ldots (A21)$$

Combining terms gives

$$GB_{gi} + \frac{GB_{gi}}{1-S_{wi}} S_{wi} - \frac{GB_{gi}}{1-S_{wi}} \bar{c}_f (p_i-p) + \frac{GB_{gi}}{1-S_{wi}} M - \frac{GB_{gi}}{1-S_{wi}} M \bar{c}_f (p_i-p)$$
$$= GB_g - (G_p-W_pR_{sw})B_g + G_{inj}B_g + \frac{GB_{gi}}{1-S_{wi}} \frac{S_{wi}}{B_{wi}} \frac{(R_{swi}-R_{sw})B_g}{5.615}$$
$$+ \frac{GB_{gi}}{1-S_{wi}} M \frac{1}{B_{wi}} \frac{(R_{swi}-R_{sw})B_g}{5.615} + \frac{GB_{gi}}{1-S_{wi}} \frac{S_{wi}}{B_{wi}} B_w$$
$$+ 5.615(W_{inj}B_w+W_e-W_pB_w) + \frac{GB_{gi}}{1-S_{wi}} M \frac{1}{B_{wi}} B_w \quad (A22)$$

Changing signs and grouping terms yields

$$G(B_g-B_{gi}) + \frac{GB_{gi}}{1-S_{wi}}\left\{S_{wi}\left[\frac{B_w+\frac{(R_{swi}-R_{sw})B_g}{5.615}}{B_{wi}} - \frac{B_{wi}}{B_{wi}}\right] + \bar{c}_f(p_i-p)\right.$$

$$\left. +M\left[\frac{B_w+\frac{(R_{swi}-R_{sw})B_g}{5.615}}{B_{wi}} - \frac{B_{wi}}{B_{wi}}\right] + M\,\bar{c}_f(p_i-p)\right\} \quad \text{(A23)}$$

$$= (G_p-W_pR_{sw}-G_{inj})B_g + 5.615\left(W_p-W_{inj}-\frac{W_e}{B_w}\right)B_w$$

Defining the total water-gas formation volume factor B_{tw},

$$B_{tw} = B_w + \frac{(R_{swi}-R_{sw})B_g}{5.615} \quad \text{(A24)}$$

and noting that $B_{twi}=B_{wi}$ gives

$$G(B_g-B_{gi}) + \frac{GB_{gi}}{1-S_{wi}}\left[S_{wi}\left(\frac{B_{tw}-B_{twi}}{B_{twi}}\right)+\bar{c}_f(p_i-p)\right.$$

$$\left. + M\left(\frac{B_{tw}-B_{twi}}{B_{twi}}\right) + M\,\bar{c}_f(p_i-p)\right] \quad \text{(A25)}$$

$$= (G_p-W_pR_{sw}-G_{inj})B_g + 5.615\left(W_p-W_{inj}-\frac{W_e}{B_w}\right)B_w$$

Defining the cumulative total water-gas compressibility $\bar{c}_{tw}$,

$$\bar{c}_{tw} = \frac{(B_{tw}-B_{twi})}{B_{twi}}\frac{1}{(p_i-p)} \quad \text{(A26)}$$

gives

$$G(B_g-B_{gi}) + GB_{gi}\left[\frac{S_{wi}\bar{c}_{tw}+\bar{c}_f}{1-S_{wi}}(p_i-p)\right.$$

$$\left. + \frac{M(\bar{c}_{tw}+\bar{c}_f)}{1-S_{wi}}(p_i-p)\right] \quad \text{(A27)}$$

$$= (G_p-W_pR_{sw}-G_{inj})B_g+5.615\left(W_p-W_{inj}-\frac{W_e}{B_w}\right)B_w$$

Defining an cumulative effective compressibility $\bar{c}_e$

$$\bar{c}_e = \frac{S_{wi}\bar{c}_{tw}+\bar{c}_f+M(\bar{c}_{tw}+\bar{c}_f)}{1-S_{wi}} \quad \text{(A28)}$$

gives

$$G(B_g-B_{gi}) + GB_{gi}[\bar{c}_e(p_i-p)]$$

$$= B_g\left[G_p-G_{inj}+W_pR_{sw}+\frac{5.615}{B_g}(W_pB_w-W_{inj}B_w-W_e)\right] \quad \text{(A29)}$$

Dividing through by GB_{gi} and expressing $B_g=(p_{sc}/T_{sc})(zT/p)$ gives the final form of the material balance

$$(p/z)\left[1-\bar{c}_e(p_i-p)\right] =$$

$$(p/z)_i\left\{1-\frac{1}{G}\left[G_p-G_{inj}+W_pR_{sw}+\frac{5.615}{B_g}(W_pB_w-W_{inj}B_w-W_e)\right]\right\} \quad \text{(A30)}$$

The p/z-cumulative plot including all terms would consider $(p/z)[1-\bar{c}_e(p_i-p)]$ versus the entire production/injection term Q

$$(p/z)[1-\bar{c}_e(p_i-p)] = (p/z)_i - \frac{(p/z)_i}{G}Q \quad \text{(A31)}$$

with

$$Q = G_p-G_{inj}+W_pR_{sw}+\frac{5.615}{B_g}(W_pB_w-W_{inj}B_w-W_e) \quad \text{(A32)}$$

where the intercept is given by $(p/z)_i$ and the slope equals $(p/z)_i/G$. Setting $G_{inj}=W_{inj}=W_p=W_e=0$ gives the common form of the gas material balance,

$$(p/z)\left[1-\bar{c}_e(p_i-p)\right] = (p/z)_i\left[1-\frac{G_p}{G}\right] \quad \text{(A33)}$$

Treating Limited Aquifers in $\bar{c}_e$ Term. The material balance thus far has considered any associated water volume expressed in terms of the M parameter. In fact M may include a limited aquifer with up to 25 times the reservoir pore volume for a system permeability greater than about 100 md, and even larger aquifer volumes for higher permeabilities. The condition that determines when a limited aquifer can be treated as part of the $\bar{c}_e$ term is outlined below. We start with the general material balance equation including a water encroachment term W_e and a $\bar{c}_e$ term that considers only non-net pay.

$$(p/z)\left[1-\bar{c}_e(p_i-p)\right] = (p/z)_i\left[1-\frac{G_p}{G}+5.615\frac{W_e}{GB_g}\right] \quad \text{(A34)}$$

$$\bar{c}_e = \frac{S_{wi}\bar{c}_{tw}+\bar{c}_f+\frac{V_{pNNP}}{V_{pR}}(\bar{c}_{tw}+\bar{c}_f)}{1-S_{wi}} \quad \text{(A35)}$$

The water encroachment term calculated by superposition is expressed,

$$W_e = B\sum_j Q_D(\Delta t_j)_D\,\Delta p_j \quad \text{(A36)}$$

where $Q_D(t_D)$ is the dimensionless cumulative influx given as a function of dimensionless time t_D and aquifer-to-reservoir radius $r_D=r_{AQ}/r_R$. Δp_j is given by p_j-p_{j-1} (in the limit for small time steps), and $\Delta t_j=t-t_{j-1}$. Assuming that permeability is reasonably high and the ratio r_{AQ}/r_R is not

too large, Q_D for the smallest time step will approach the limiting value Q_D^{∞}, and the summation can be closely approximated by

$$\sum_j Q_D(\Delta t_j)_D \Delta p_j = Q_D^{\infty}(p_i - p) \quad \ldots\ldots\ldots\ldots\ldots\ldots \quad (A37)$$

giving a simple expression for W_e which is independent of time and only dependent on reservoir pressure,

$$W_e = B\, Q_D^{\infty}(p_i - p) \quad ; \; W_e(\text{bbl}) \quad \ldots\ldots\ldots\ldots\ldots\ldots \quad (A38)$$

$$B = \frac{2\pi}{5.615}\phi r_R^2 h(\bar{c}_{tw} + \bar{c}_f) \quad \ldots\ldots\ldots\ldots\ldots\ldots \quad (A39)$$

$$Q_D^{\infty} = \frac{1}{2}\left[\left(\frac{r_{AQ}}{r_R}\right)^2 - 1\right]$$

Expressing W_e in terms of aquifer pore volume V_{pAQ},

$$W_e = \pi\left(r_{AQ}^2 - r_R^2\right)\phi h(\bar{c}_{tw} + \bar{c}_f)(p_i - p) \quad ; \quad W_e(\text{ft}^3) \quad \ldots\ldots\ldots \quad (A40)$$

$$= V_{pAQ}(\bar{c}_{tw} + \bar{c}_f)(p_i - p)$$

The material balance equation can then be written:

$$(p/z)\left[1 - \bar{c}_e(p_i - p)\right] = (p/z)_i\left[1 - \frac{G_p}{G}\right] + (p/z)_i\frac{W_e}{GB_g}5.615 \quad \ldots \quad (A41)$$

and simplified in a form where the $\bar{c}_e$ term includes the aquifer contribution to pressure support,

$$(p/z)_i\frac{W_e}{GB_g} = (p/z)_i\frac{W_e}{G}\frac{T_{sc}}{P_{sc}T}(p/z)$$

$$(p/z)_i\frac{W_e}{GB_g} = (p/z)\frac{W_e}{GB_g} \quad ; \; GB_g = V_{pR}(1 - S_{wi}) \quad \ldots\ldots\ldots \quad (A42)$$

$$(p/z)_i\frac{W_e}{GB_g} = (p/z)\frac{V_{pAQ}(\bar{c}_{tw} + \bar{c}_f)(p_i - p)}{V_{pR}(1 - S_{wi})}$$

Rearranging we arrive at the general form of the material balance (without water production and gas/water injection terms):

$$(p/z)\left[1 - \bar{c}_e(p_i - p)\right] = (p/z)_i\left[1 - \frac{G_p}{G}\right] \quad \ldots\ldots\ldots\ldots\ldots \quad (A43)$$

where

$$\bar{c}_e = \frac{S_{wi}\bar{c}_w + \bar{c}_f + \left[\frac{V_{pNNp}}{V_{pR}} + \frac{V_{pAQ}}{V_{pR}}\right](\bar{c}_w + \bar{c}_f)}{1 - S_{wi}} \quad \ldots\ldots\ldots \quad (A44)$$

$$M = \frac{V_{pNNP} + V_{pAQ}}{V_{pR}} = \frac{V_{pA}}{V_{pR}} \quad \ldots\ldots\ldots\ldots\ldots\ldots \quad (A45)$$

$$\bar{c}_e = \frac{S_{wi}\bar{c}_{tw} + \bar{c}_f + M(\bar{c}_{tw} + \bar{c}_f)}{(1 - S_{wi})} \quad \ldots\ldots\ldots\ldots\ldots\ldots \quad (A46)$$

TABLE 1 - CALCULATION OF PORE VOLUME COMPRESSIBILITY FROM LABORATORY DATA								
Reported Laboratory Data					Calculations for p_i=9800 psia			
p_o (psia)	V_p (cm^3)	V_b (cm^3)	ϕ (%)	c_f	p (psia)	p_i-p (psi)	V_{pi}-V_p (cm^3)	$\bar{c}_f$ Eq. 5
200.0	3.420	20.530	16.70	16.50	9800	0	0.000	16.50
1000.0	3.379	20.489	16.49	13.70	9000	800	0.041	14.99
2000.0	3.337	20.447	16.32	11.40	8000	1800	0.083	13.48
3000.0	3.303	20.413	16.18	9.10	7000	2800	0.117	12.22
4000.0	3.276	20.386	16.07	6.90	6000	3800	0.144	11.08
5000.0	3.257	20.367	15.99	5.00	5000	4800	0.163	9.93
6000.0	3.243	20.353	15.93	3.80	4000	5800	0.177	8.92
7000.0	3.230	20.340	15.88	4.10	3000	6800	0.190	8.17
8000.0	3.213	20.323	15.81	7.30	2000	7800	0.207	7.76
9000.0	3.177	20.287	15.70	16.80	1000	8800	0.243	8.07
9500.0	3.144	20.254	15.50	25.80	500	9300	0.276	8.68

All compressibilities in 10^{-6} psi^{-1}.

TABLE 2 - COMPARISON OF c_f FOR NORMAL PRESSURE AND OVERPRESSURED CONDITIONS

Sample	Initial Porosity (%)	Normal Pressure c_{fi} (psi^{-1})	Over-Pressured c_{fi} (psi^{-1})
Gulf Coast Sandstones			
Sample 1	13	4.8	6.4
Sample 2	20	4.4	16.5
North Sea Chalk			
Sample 9 (pore collapse)	32	18.3	7.9
Sample 10 (pore collapse)	30	20.1	7.4
Von Gonten			
Sample 9A	11	3.0	6.0
Sample 4A	22	4.6	9.2
Sample 7A	26	5.9	7.2
Sample 3A	28	8.6	10.6
Sample 6A	25	7.8	8.6

Normal Pressured is 0.5 psi/ft x Depth ;
Overpressured is 0.8 psi/ft x Depth. Depth Used is 10,000 ft.

TABLE 3A - EXAMPLE CALCULATION OF TOTAL WATER CUMULATIVE COMPRESSIBILITY FOR THE ANDERSON "L" RESERVOIR

Pressure psia	B_w bbl/STB	R_{sw} scf/STB	Z_g	B_g ft3/scf	B_{tw} bbl/STB	c_{tw} 10^{-6} psi^{-1}
9510	1.0560	31.8	1.4401	0.00282	1.056	2.40
9000	1.0569	31.0	1.3923	0.00288	1.057	2.43
8000	1.0586	29.2	1.2991	0.00303	1.060	2.51
7000	1.0604	27.2	1.2072	0.00322	1.063	2.65
6000	1.0621	25.0	1.1176	0.00347	1.066	2.78
5000	1.0638	22.5	1.0325	0.00385	1.070	2.98
4000	1.0654	19.6	0.9562	0.00446	1.075	3.28
3000	1.0669	16.1	0.8977	0.00558	1.083	3.86
2000	1.0681	11.8	0.8744	0.00815	1.097	5.19
1500	1.0686	9.3	0.8832	0.01098	1.113	6.69
1000	1.0691	6.5	0.9078	0.01693	1.145	9.95
750	1.0692	5.0	0.9258	0.02302	1.179	13.30
500	1.0693	3.3	0.9472	0.03533	1.249	20.24
250	1.0694	1.6	0.9708	0.07242	1.459	41.20
100	1.0694	0.5	0.9835	0.18341	2.092	104.23
14.7	1.0694	0.0	1.0000	1.26860	8.254	717.86

B_w and R_{sw} were calculated from the Peng-Robinson EOS with volume translation using binary interaction parameters that are functions of temperature and salinity (28,000 PPM for this example); the gas Z-factor was calculated from the Standing-Katz correlation.

TABLE 3B - EXAMPLE CALCULATION OF TOTAL WATER CUMULATIVE COMPRESSIBILITY FOR THE ELLENBURGER RESERVOIR WITH INITIAL 28% CO_2 CONCENTRATION

Pressure psia	B_w bbl/STB	R_{sw} scf/STB	Z_g	B_g ft3/scf	B_{tw} bbl/STB	c_{tw} 10^{-6} psi^{-1}
6675	1.0761	67.5	1.0464	0.00292	1.076	2.75
6000	1.0765	64.5	0.9962	0.00310	1.078	2.83
5000	1.0768	59.5	0.9262	0.00345	1.082	3.12
4000	1.0770	53.5	0.8732	0.00407	1.087	3.84
3000	1.0767	46.1	0.8493	0.00528	1.097	5.24
2500	1.0764	41.5	0.8513	0.00635	1.106	6.61
2000	1.0758	36.1	0.8638	0.00805	1.121	8.89
1750	1.0754	33.0	0.8742	0.00932	1.133	10.67
1500	1.0749	29.6	0.8872	0.01103	1.149	13.15
1250	1.0743	25.8	0.9028	0.01347	1.174	16.83
1000	1.0735	21.6	0.9208	0.01717	1.214	22.56
750	1.0727	16.9	0.9408	0.02339	1.284	32.53
500	1.0716	11.7	0.9621	0.03588	1.428	52.99
250	1.0704	5.8	0.9833	0.07335	1.876	115.75
100	1.0695	1.9	0.9946	0.18548	3.236	305.33
14.7	1.0689	0.0	1.0000	1.26860	16.319	2126.80

B_w and R_{sw} were calculated from the Peng-Robinson EOS with volume translation using binary interaction parameters that are functions of temperature and salinity (50,000 PPM for this example); the gas Z-factor was calculated from the Standing-Katz correlation.

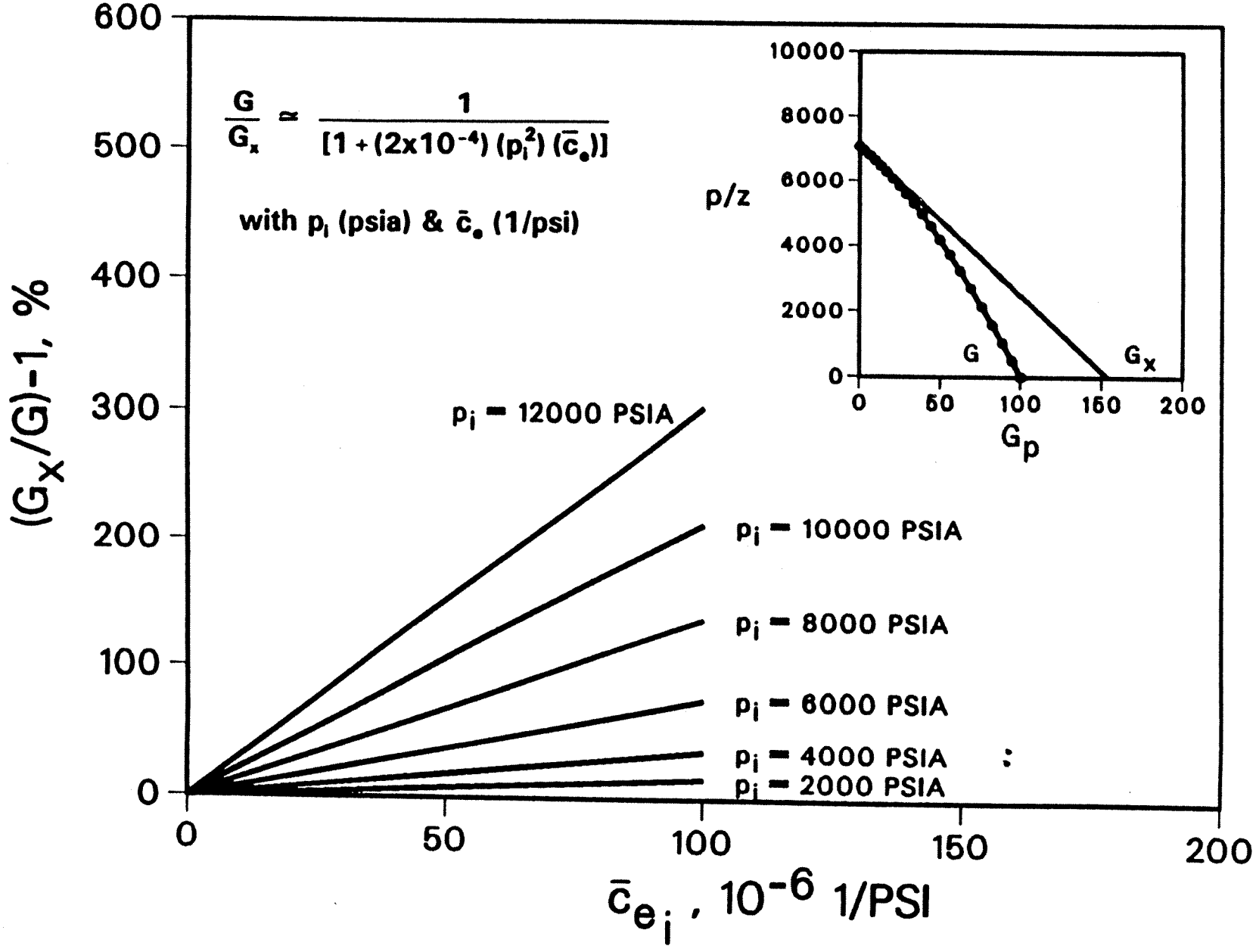

Fig. 1 Effect of p_i and $\bar{c}_e$ on Overestimating G

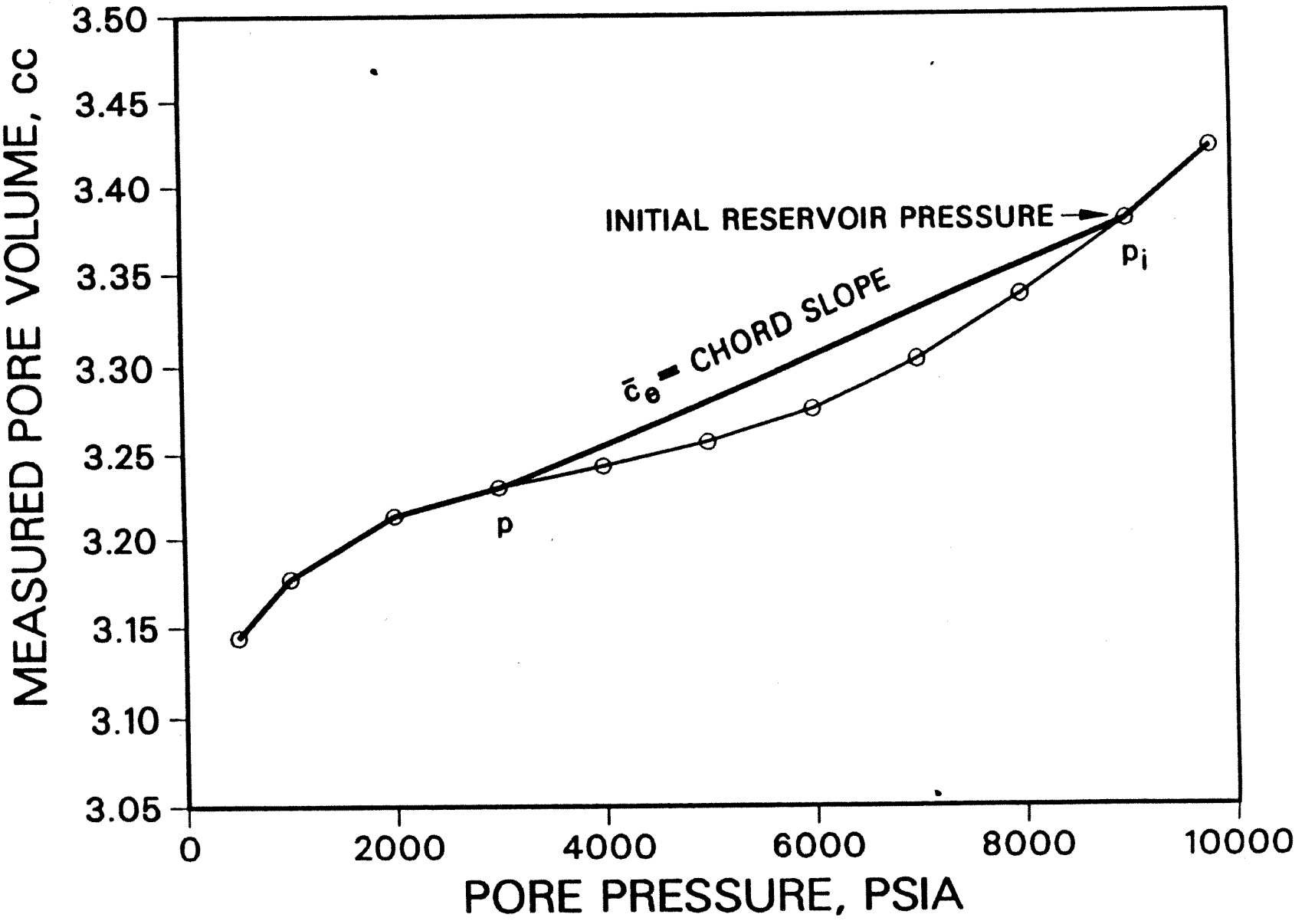

Fig. 2 Cumulative Pore Volume Compressibility as a Chord Slope

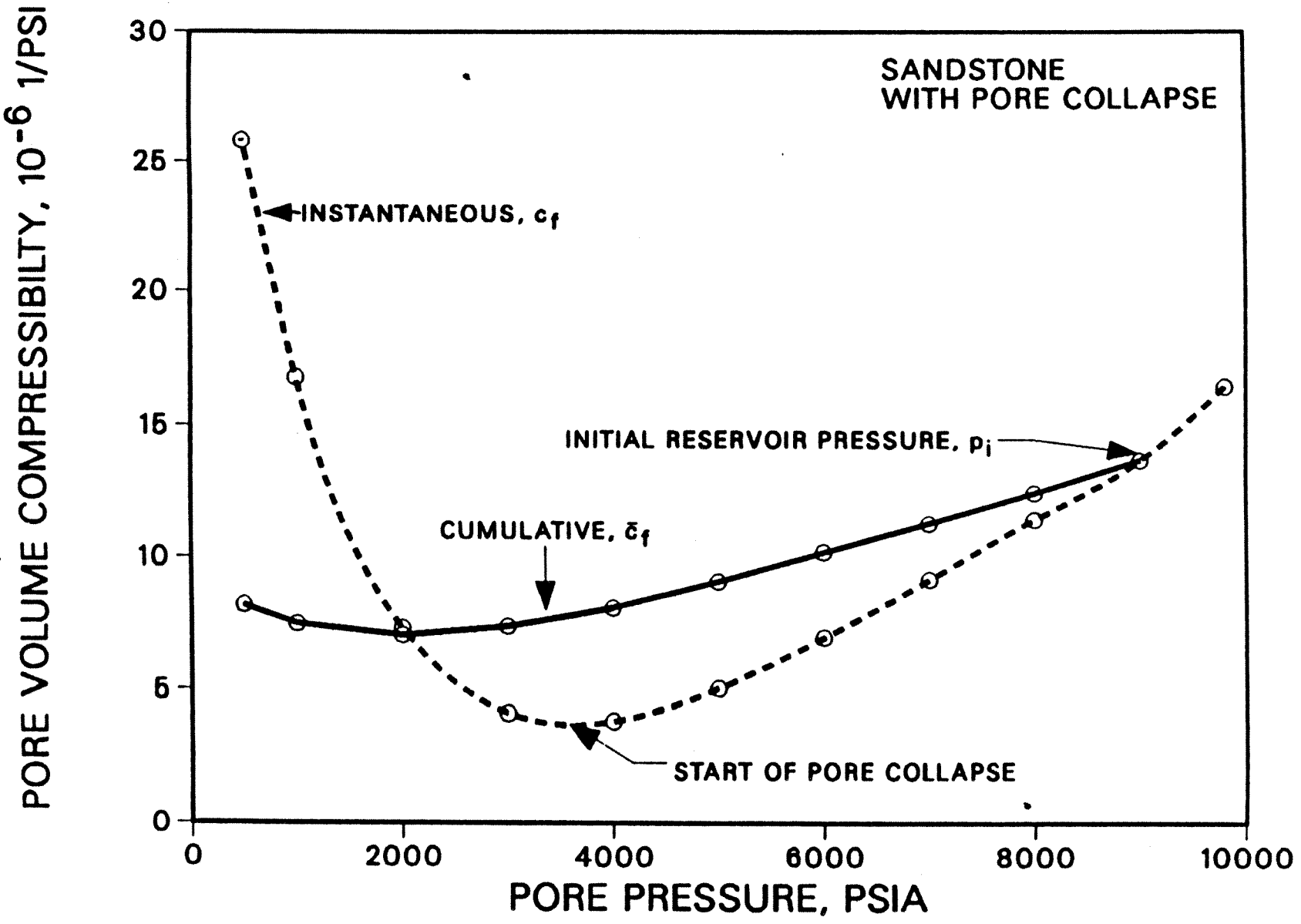

Fig. 3 Cumulative and Instantaneous c_f vs p for a Sandstone With Pore Collapse

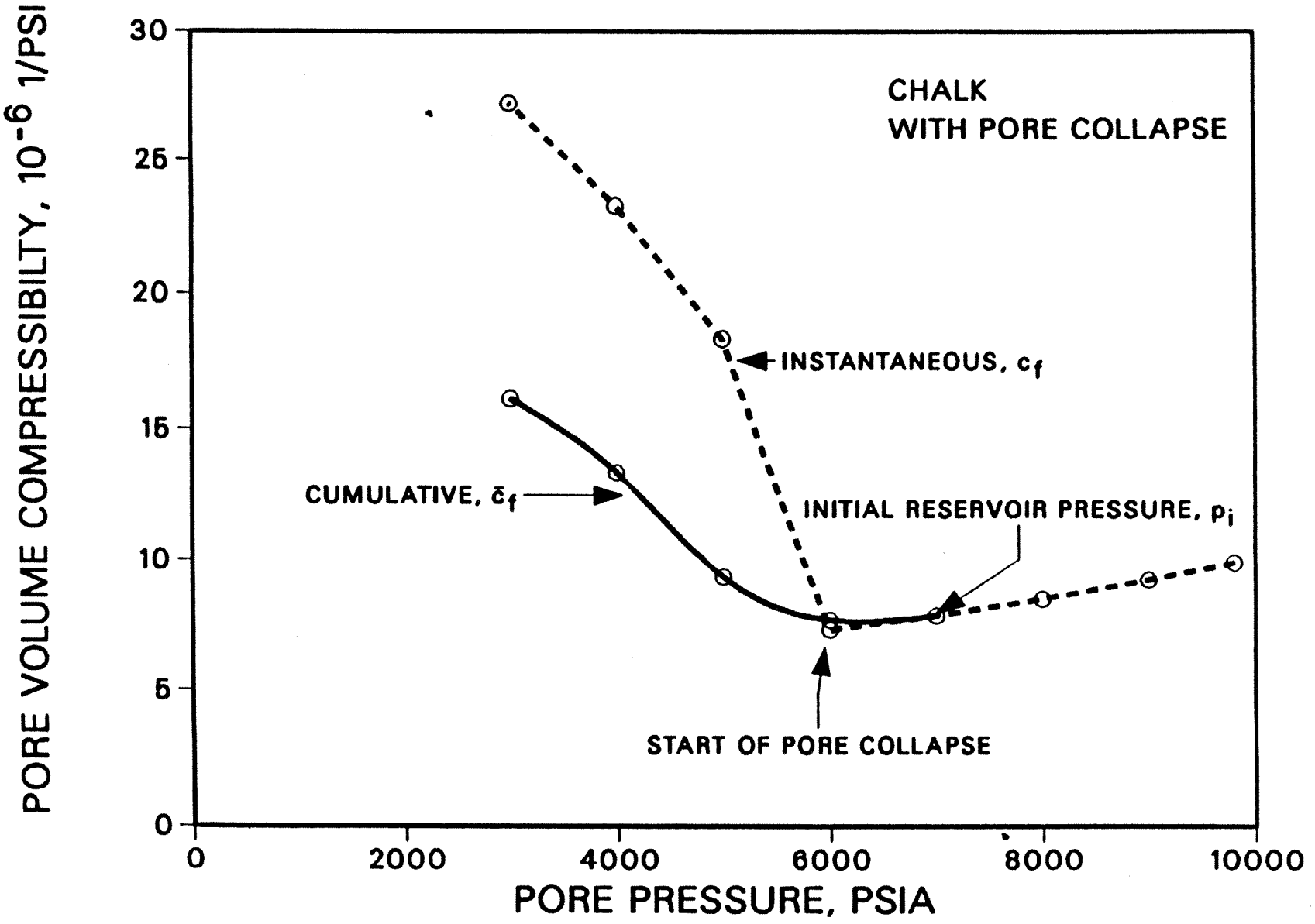

Fig. 4 Cumulative and Instantaneous c_f vs p for a Chalk With Pore Collapse

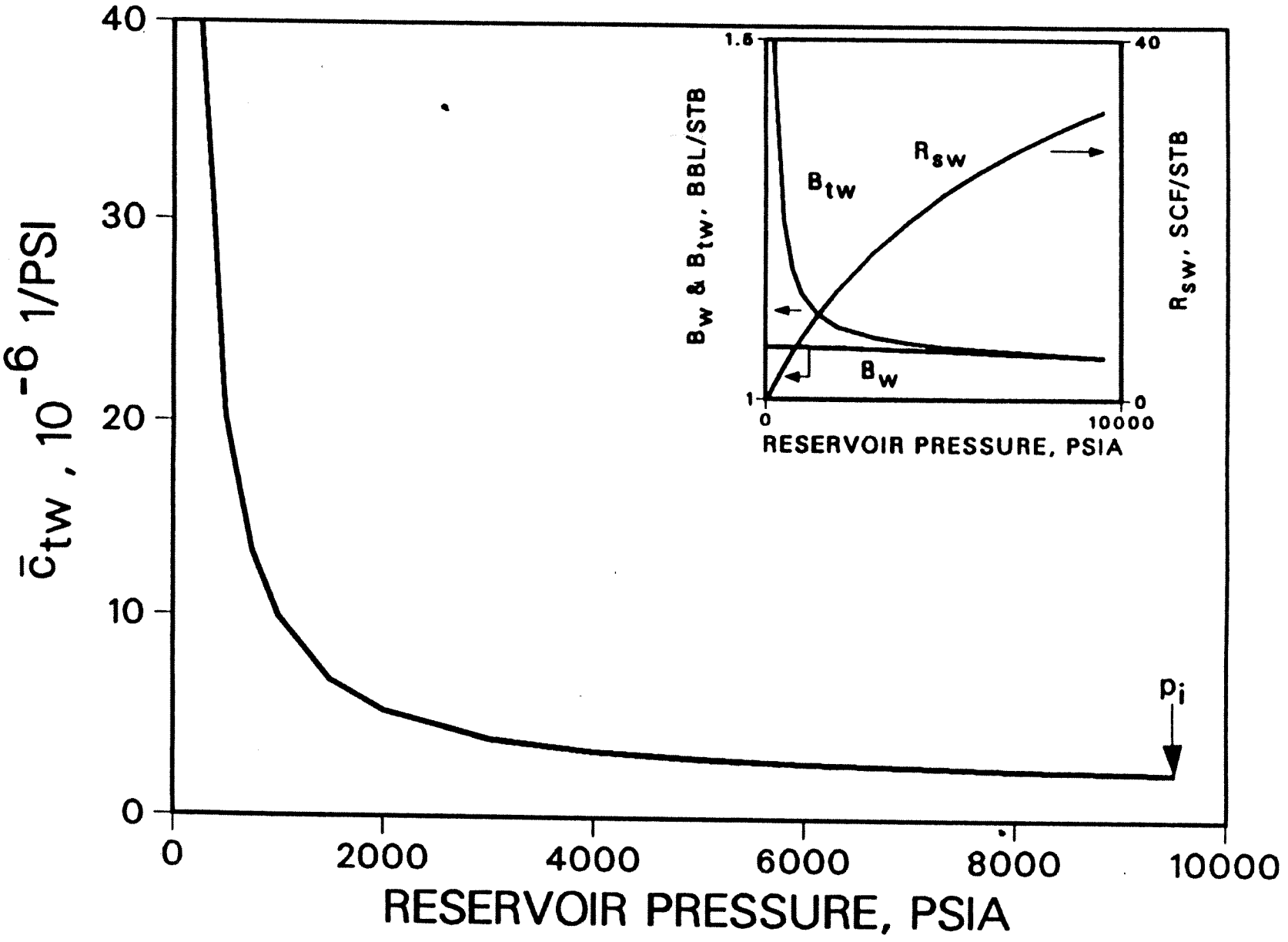

Fig. 5 Cumulative Total Water Compressibility, $\bar{c}_{tw}$, vs p

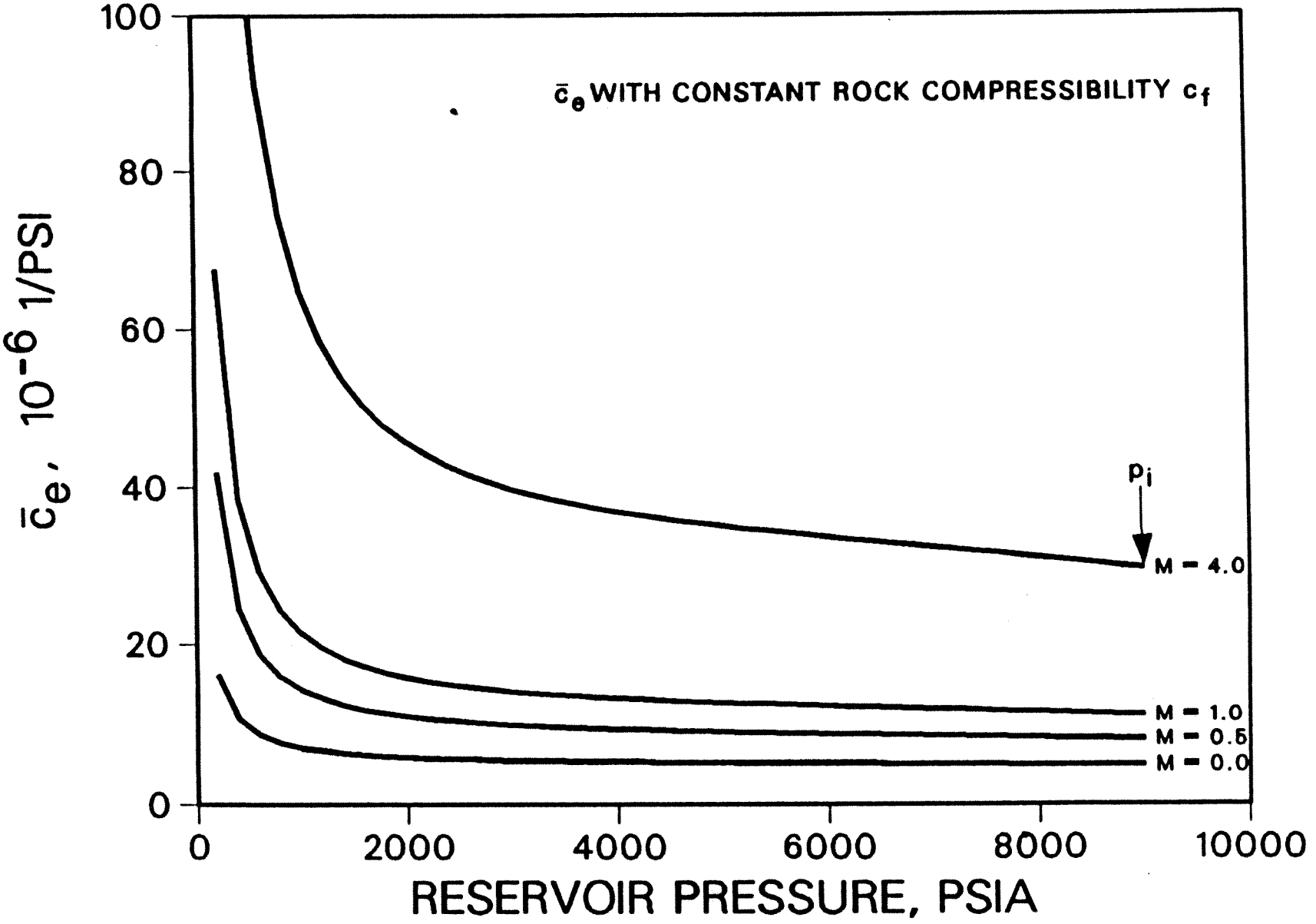

Fig. 6 Cumulative Effective Compressibility vs p at Various M Ratios

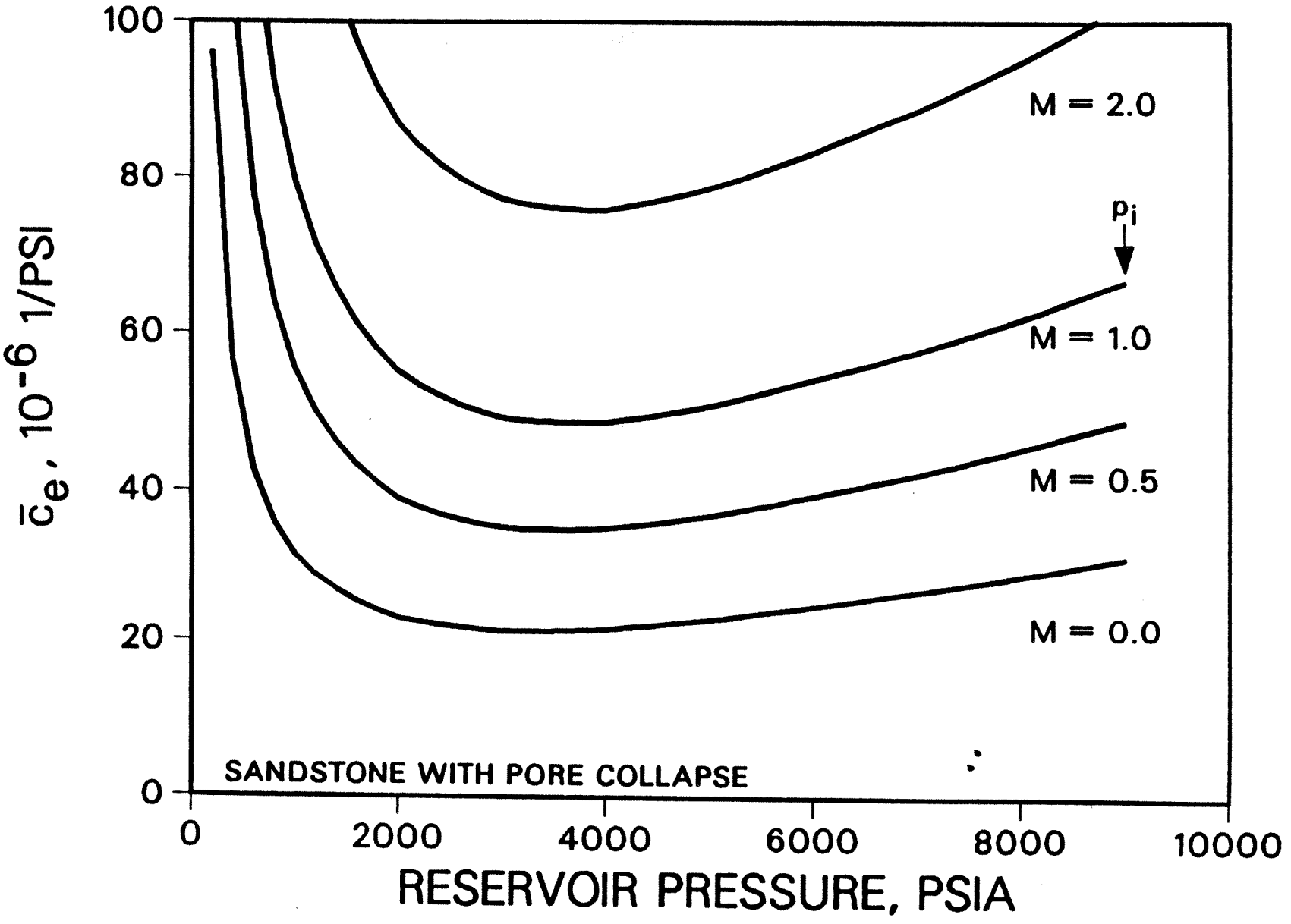

Fig. 7 Cumulative Effective Compressibility vs p for a Sandstone W/Pore Collapse

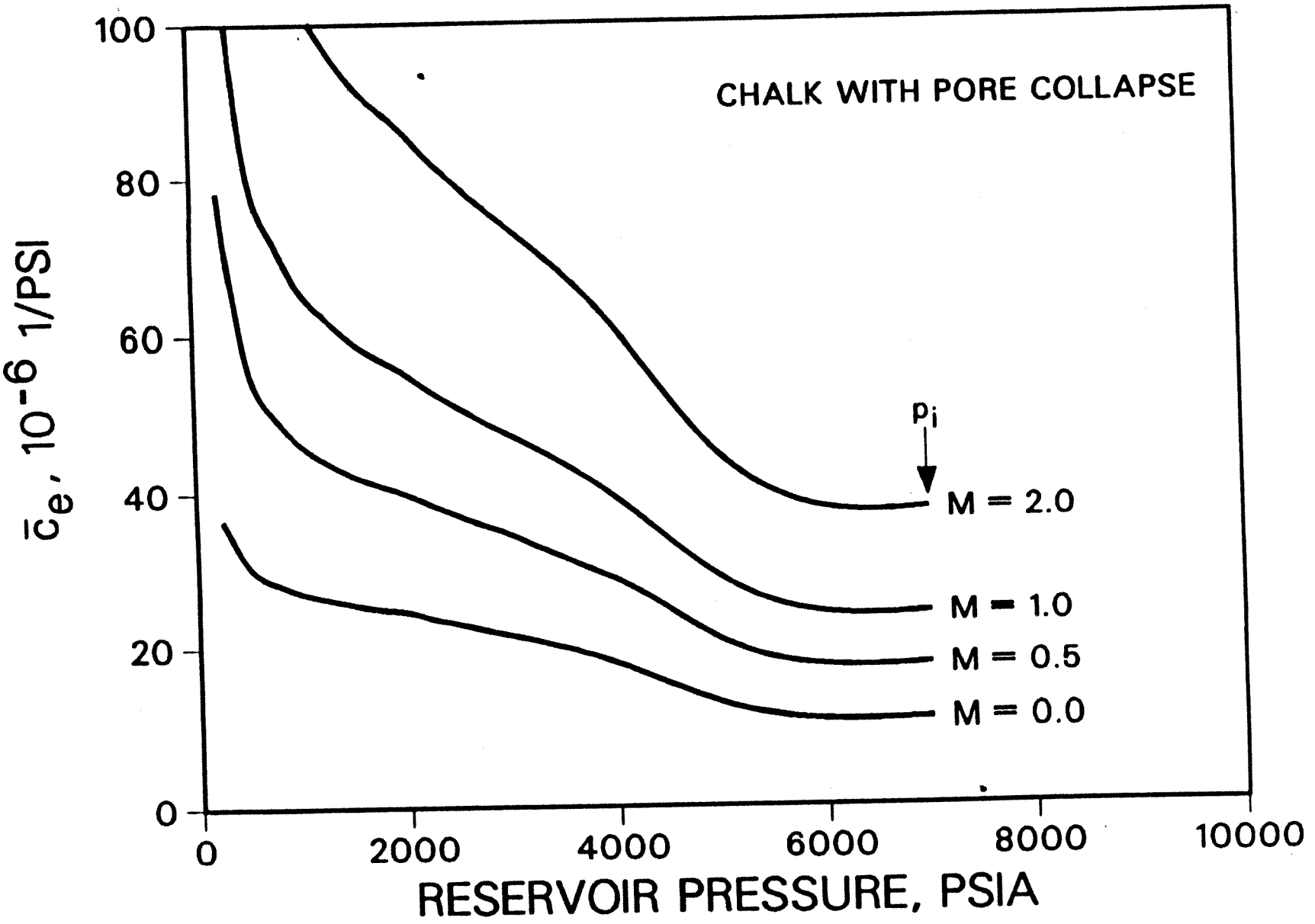

Fig. 8 Cumulative Effective Compressibility vs p for a Chalk W/Pore Collapse

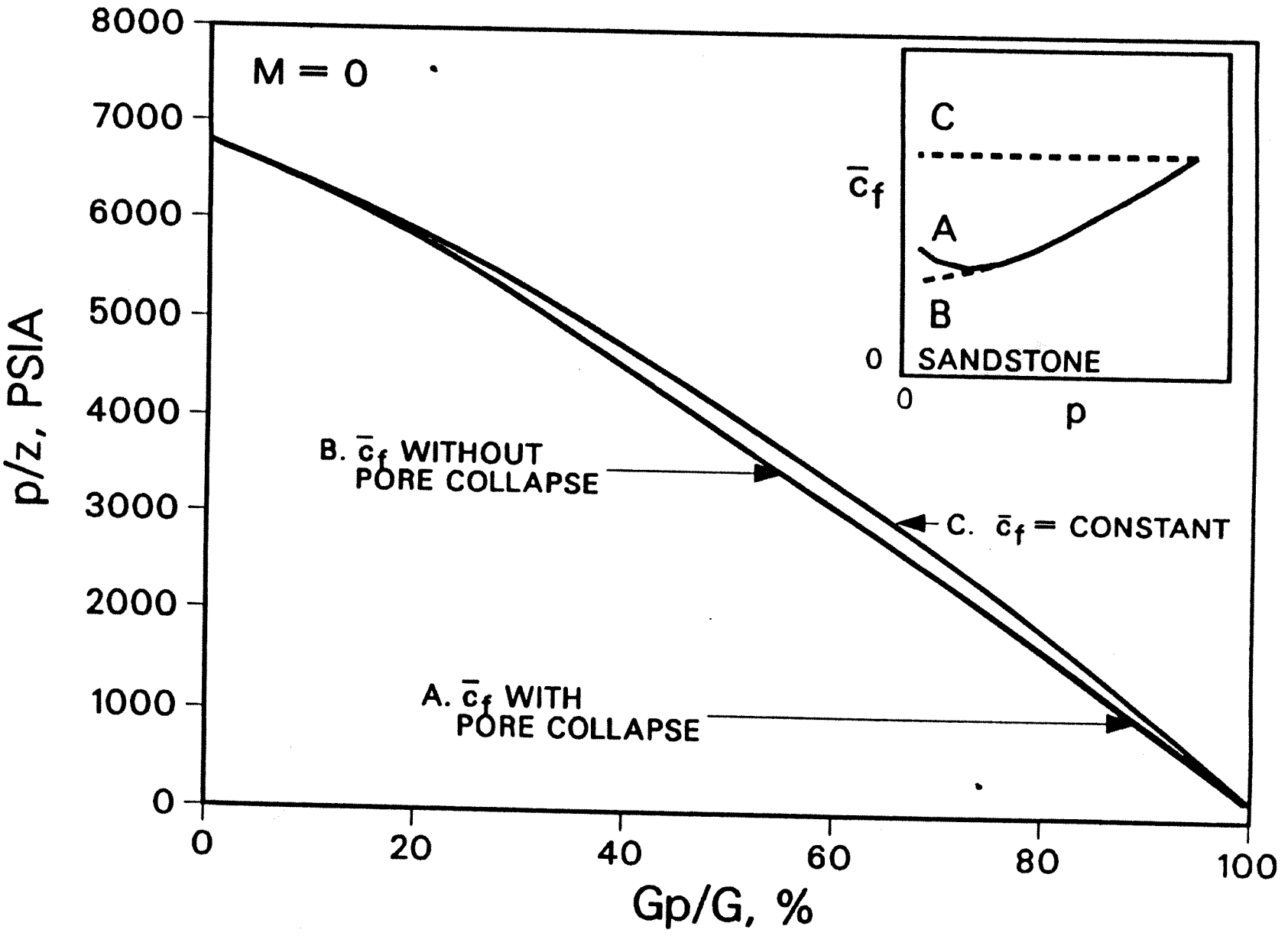

Fig. 9 Effect on p/Z vs G_p With and Without Pore Collapse, Sandstone

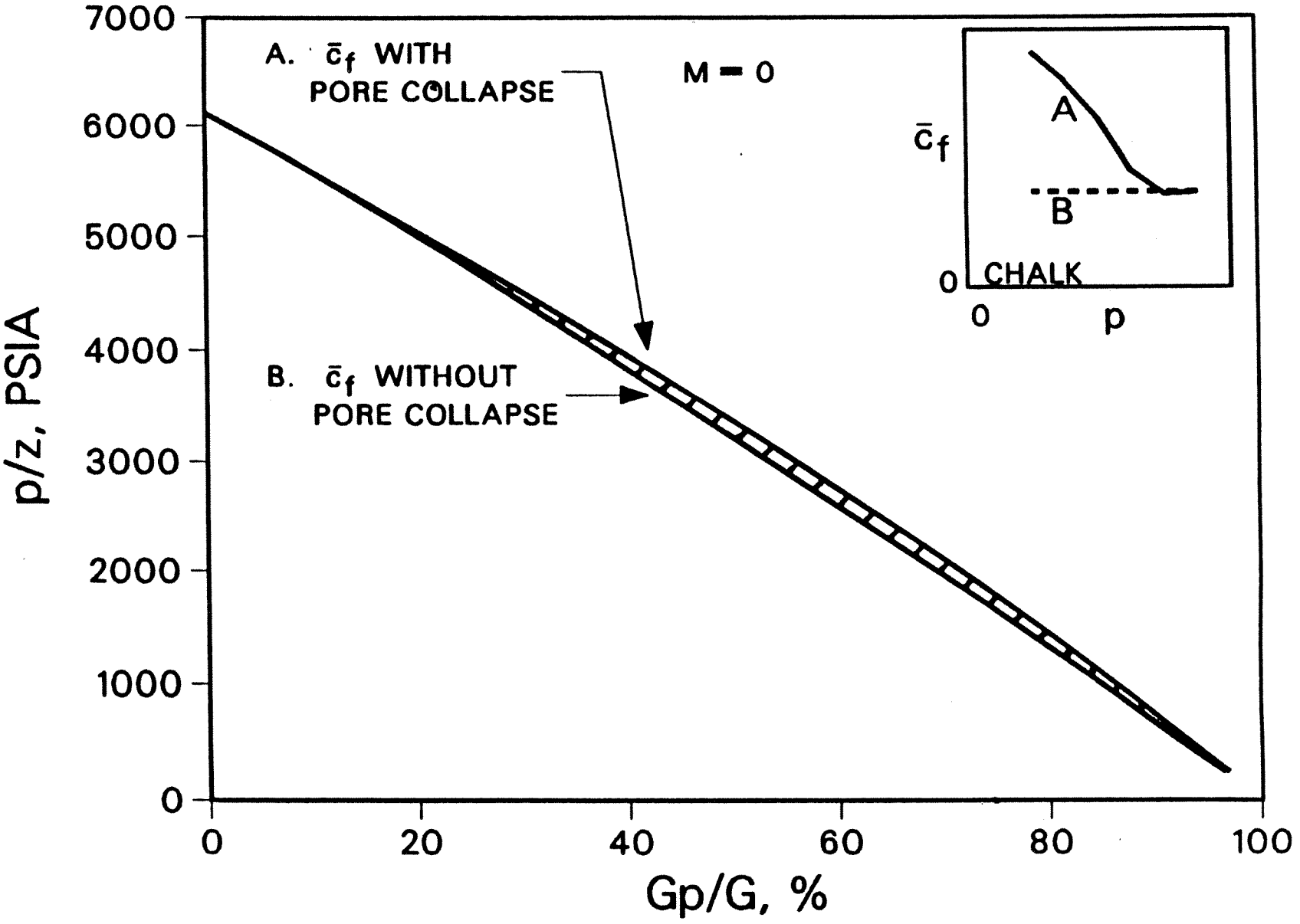

Fig. 10 Effect on p/Z vs G_p With and Without Pore Collapse, Chalk

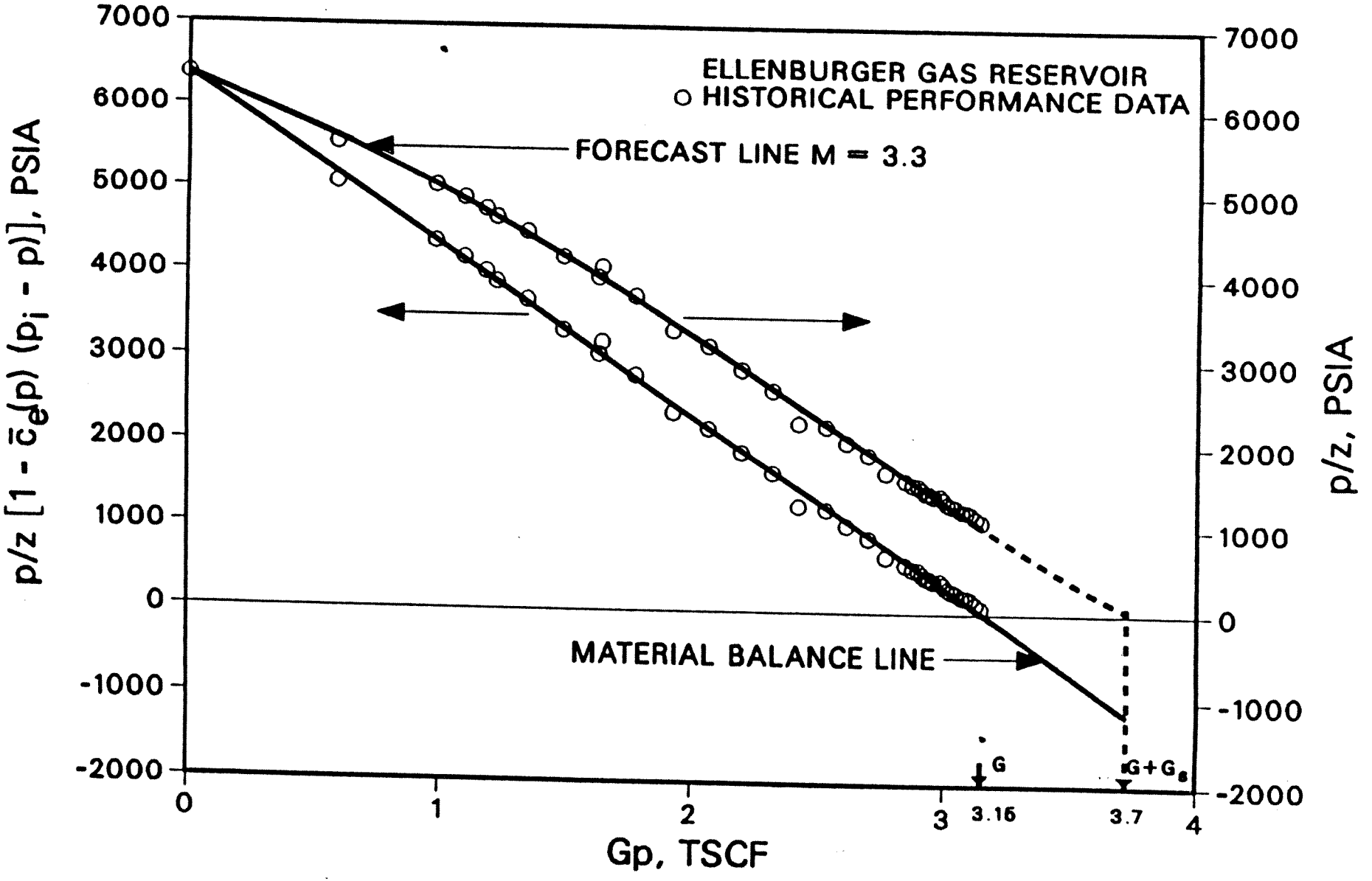

Fig. 11 Pressure vs Cumulative Production, Ellenburger Gas Reservoir

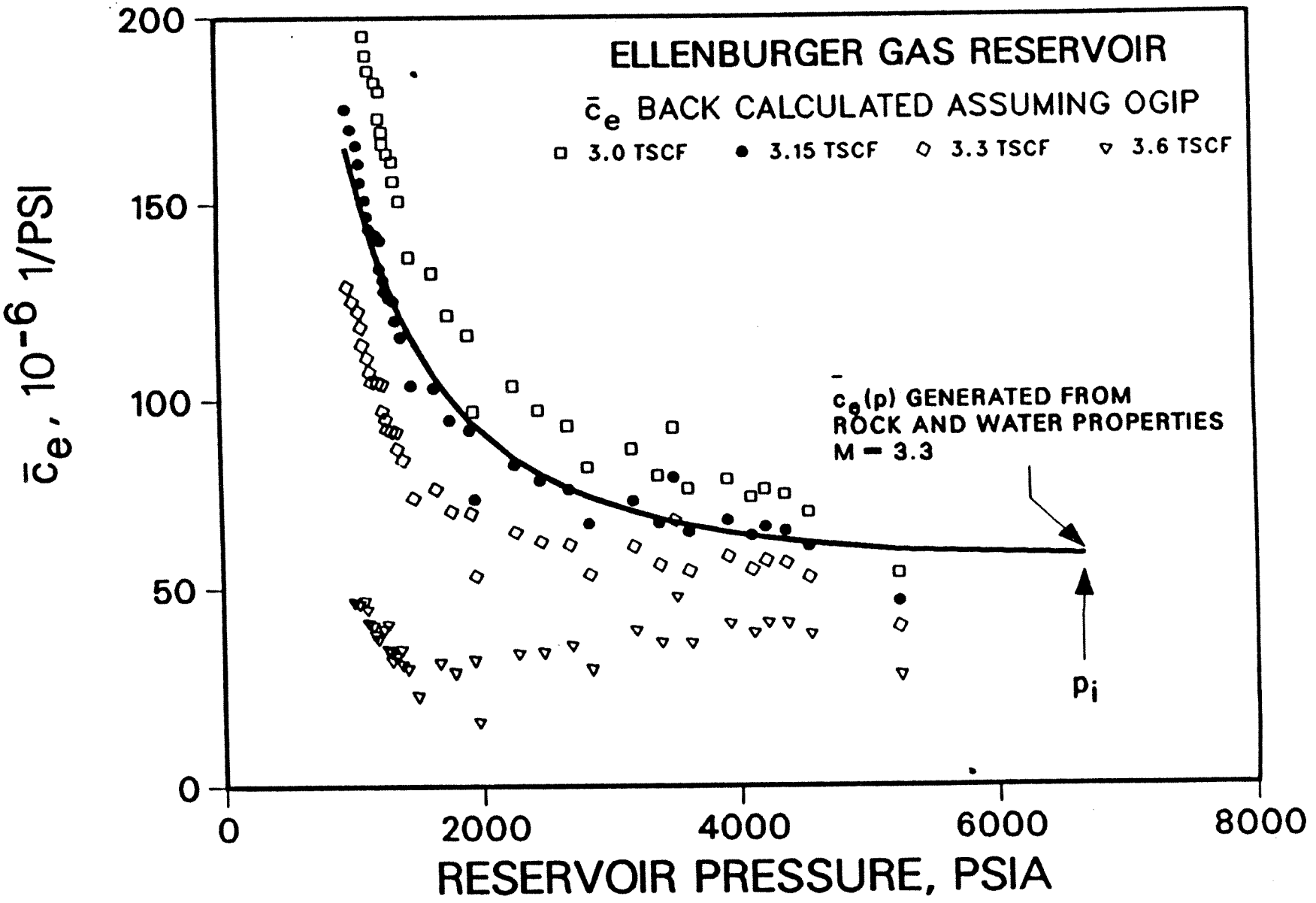

Fig. 12 Backcalculated $\bar{c}_e$ vs p at Various OGIP, Ellenburger Gas Reservoir

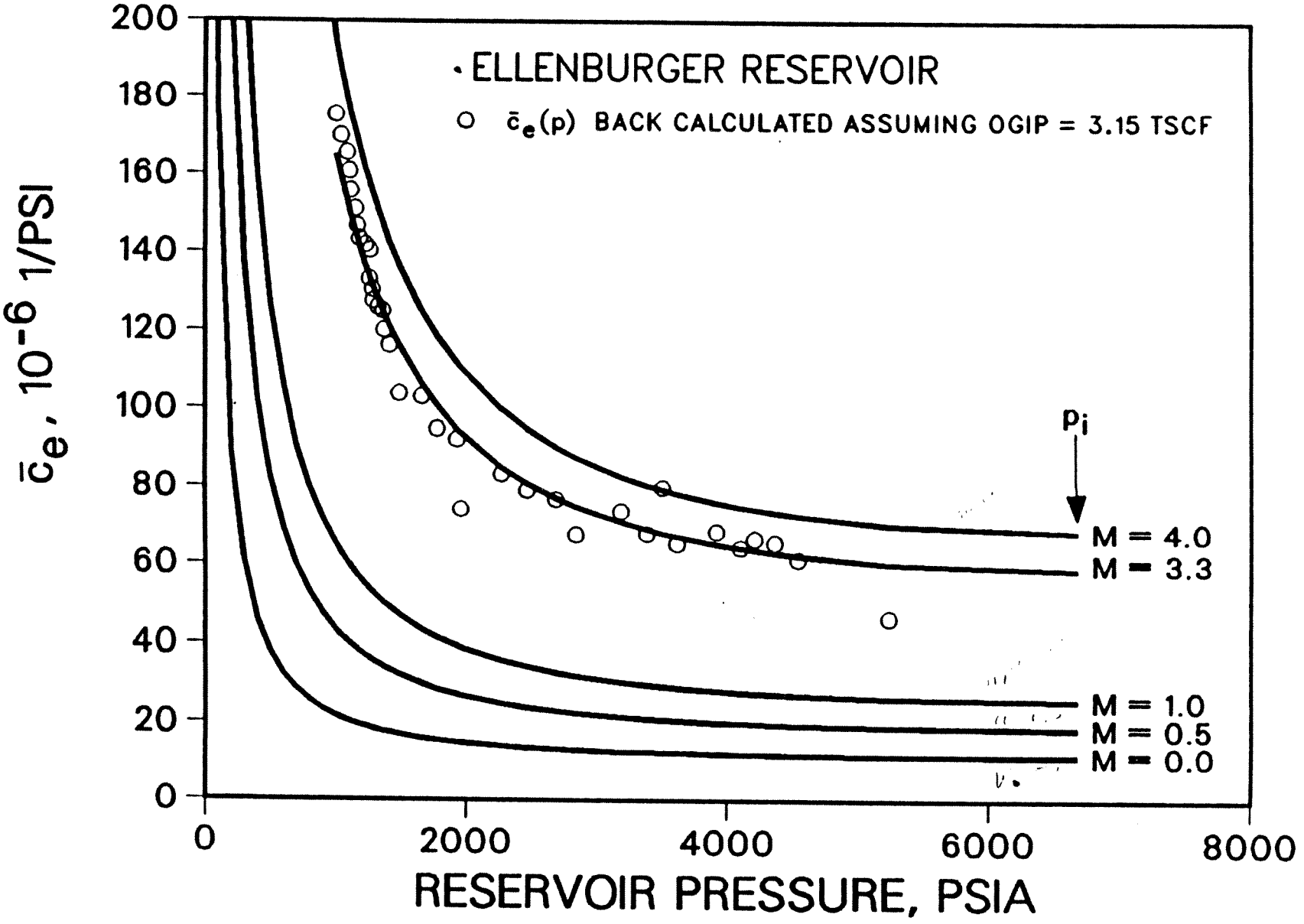

Fig. 13 Matching Backcalculated $\bar{c}_e$ to Generated $\bar{c}_e$ Curves, Ellenburger Gas Reservoir

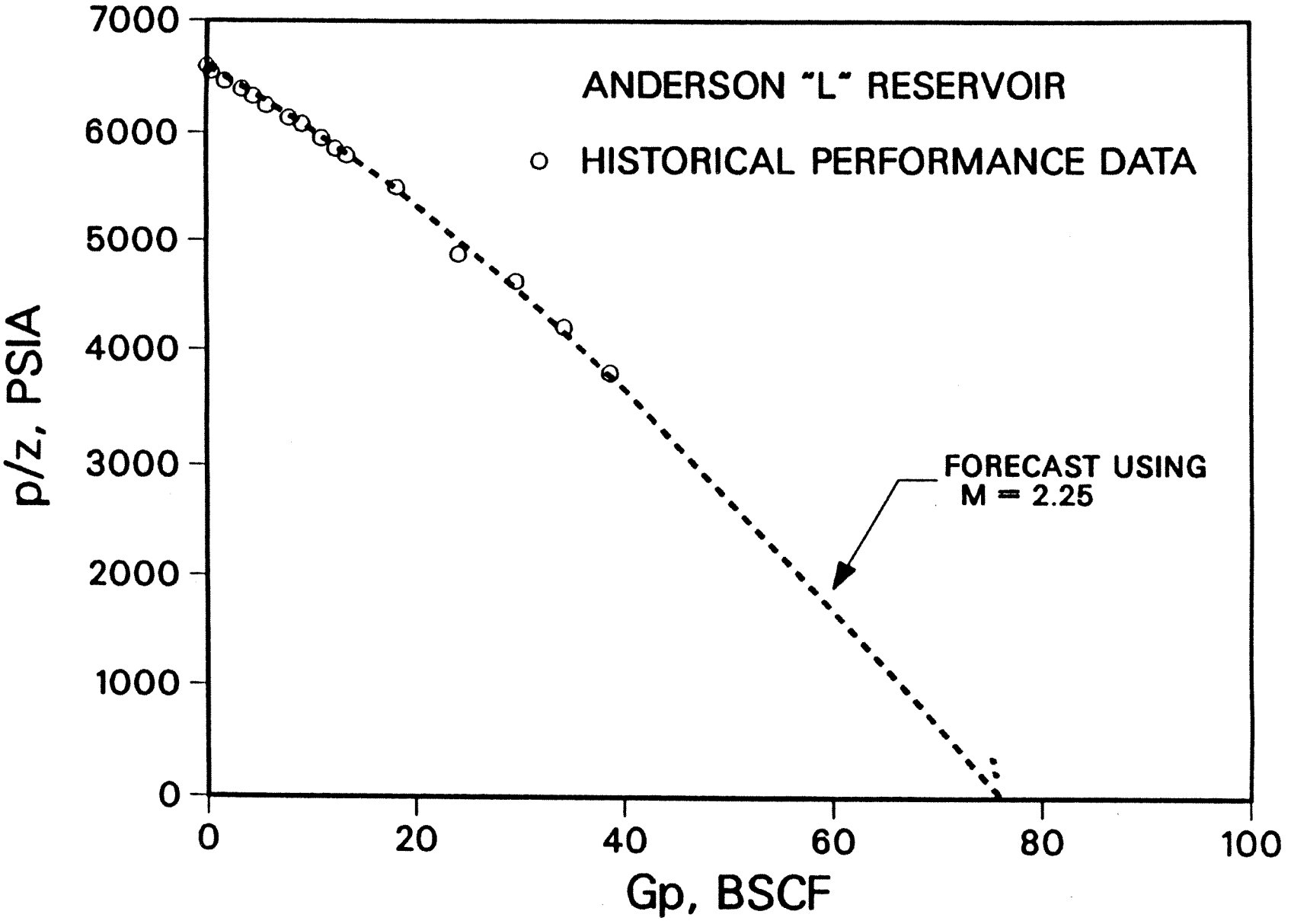

Fig. 14 p/Z vs Cumulative Production, Anderson "L" Reservoir

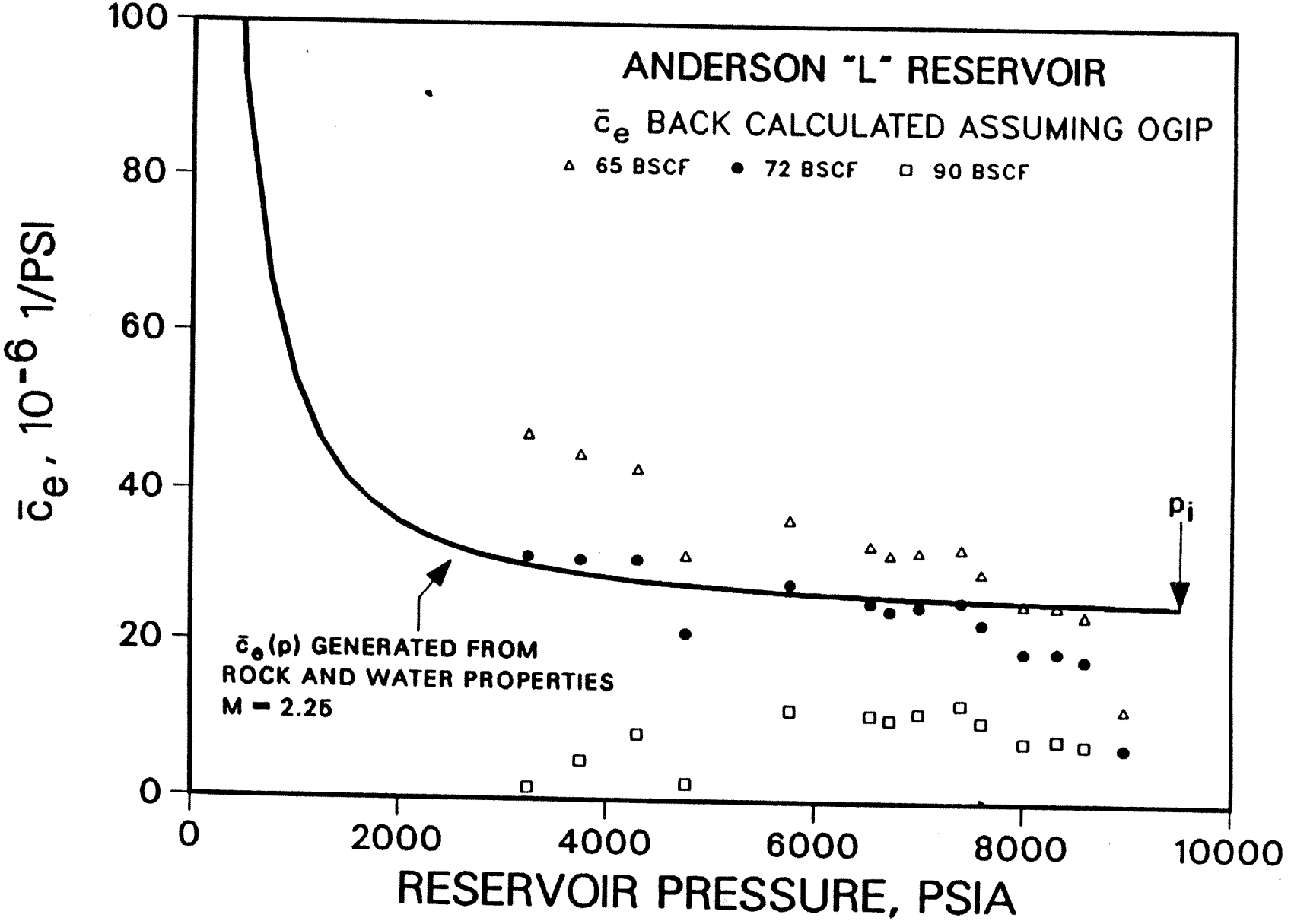

Fig. 15 Backcalculated $\bar{c}_e$ vs p at Various OGIP, Anderson "L" Reservoir

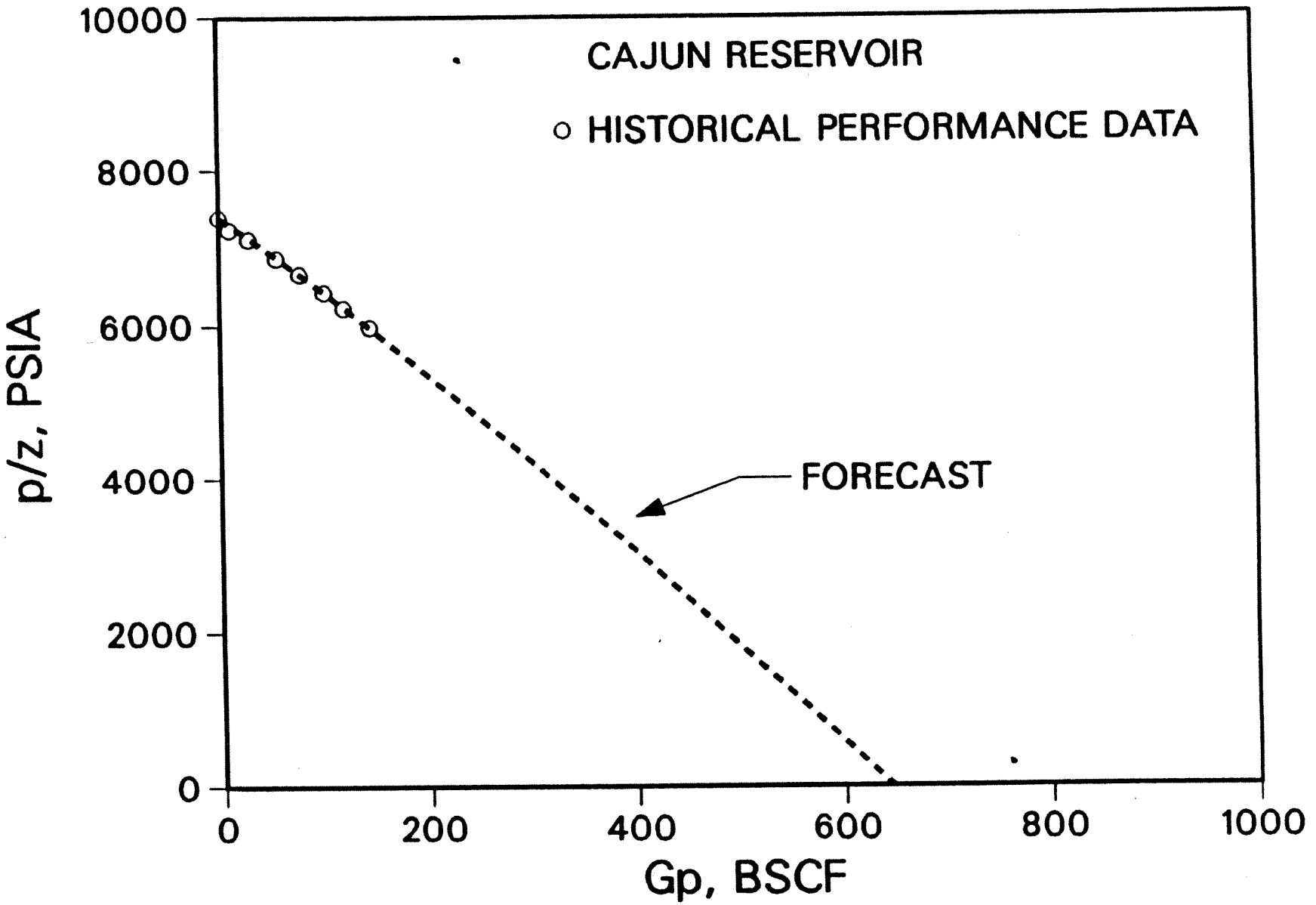

Fig. 16 p/Z vs Cumulative Production, Cajun Reservoir

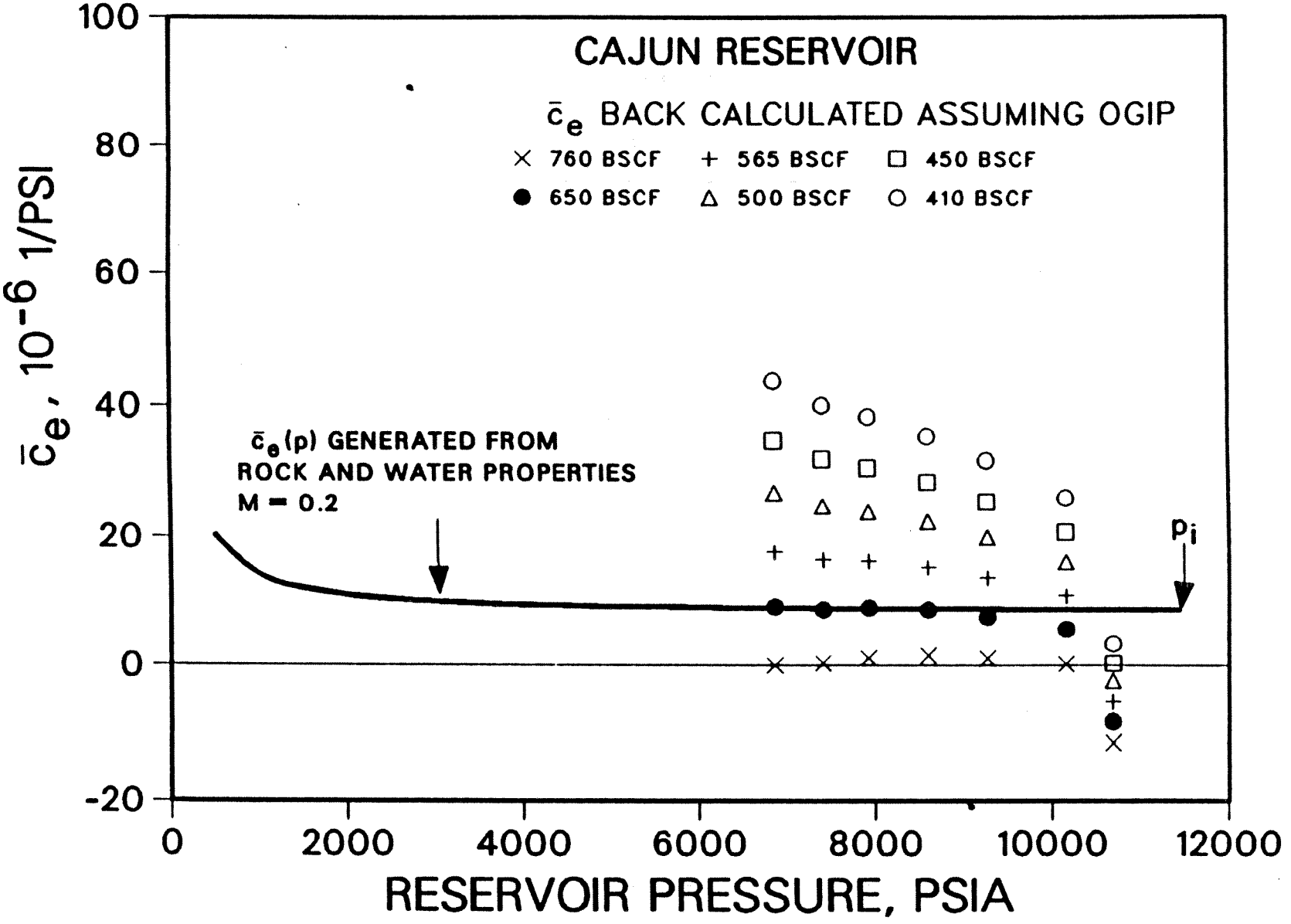

Fig. 17 Backcalculated $\bar{c}_e$ vs p at Various OGIP, Cajun Reservoir

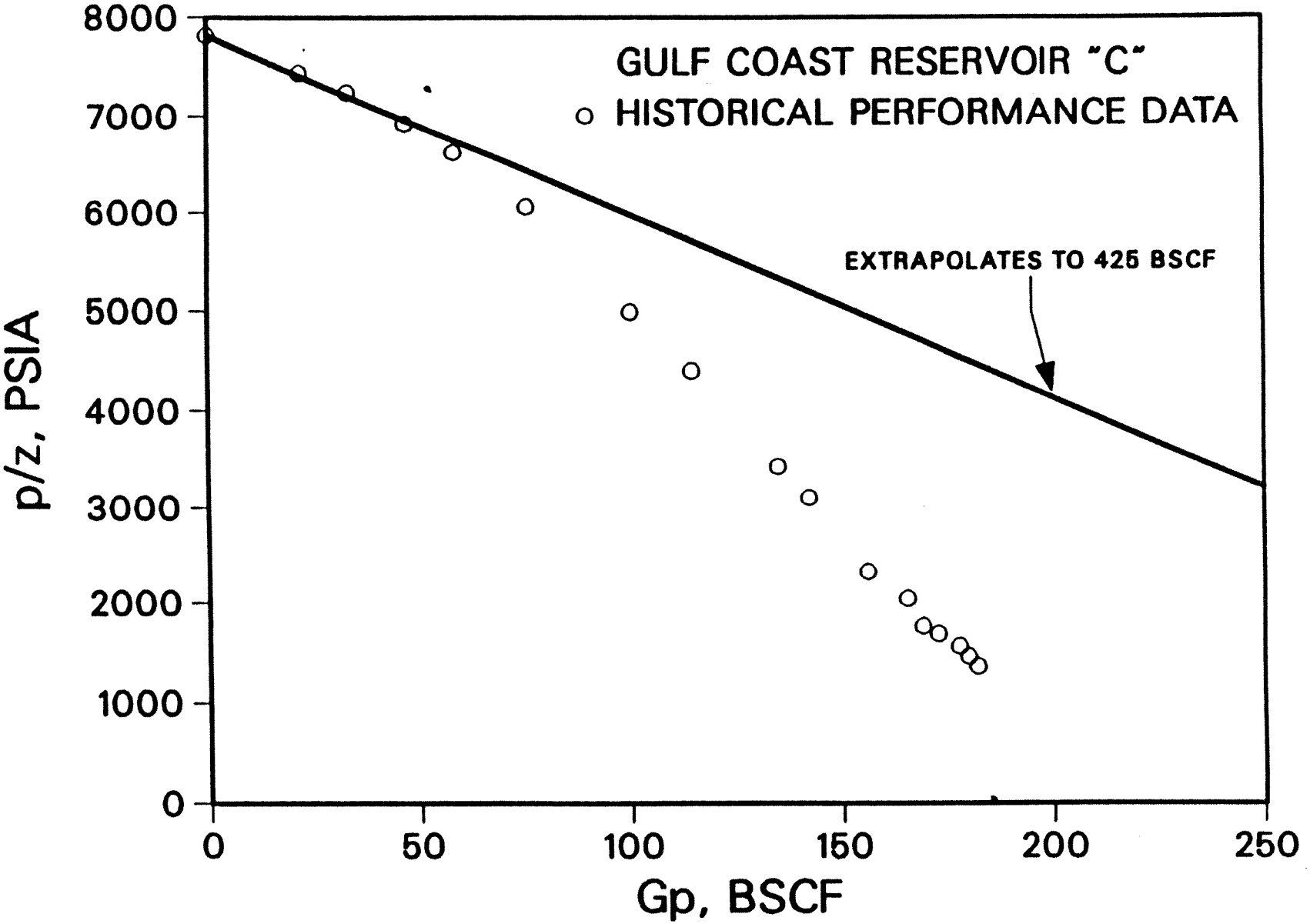

Fig. 18 p/z vs Cumulative Production, Gulf Coast Reservoir "C"

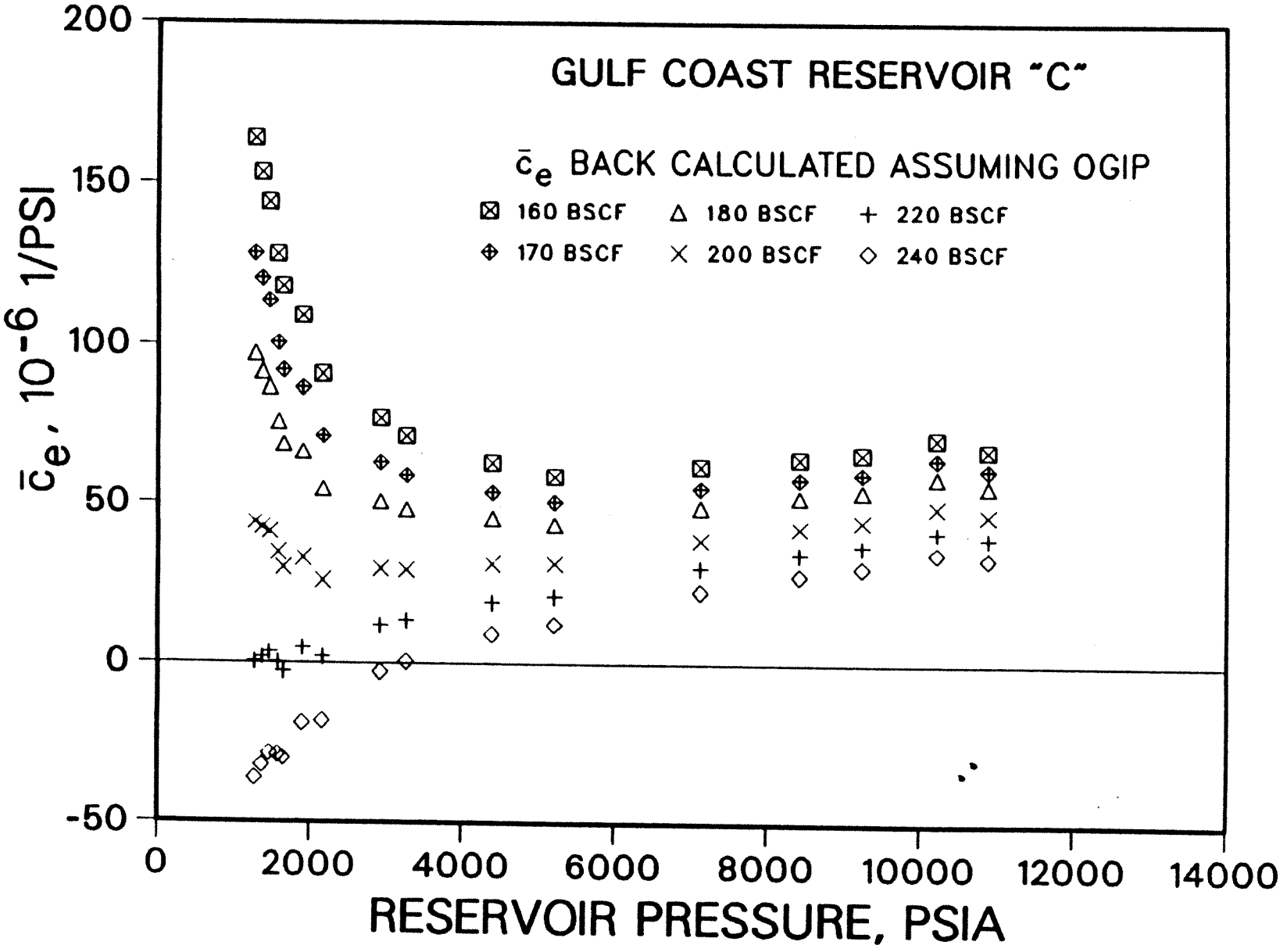

Fig. 19 Backcalculated $\bar{c}_e$ vs p at Various OGIP, Gulf Coast Reservoir "C"

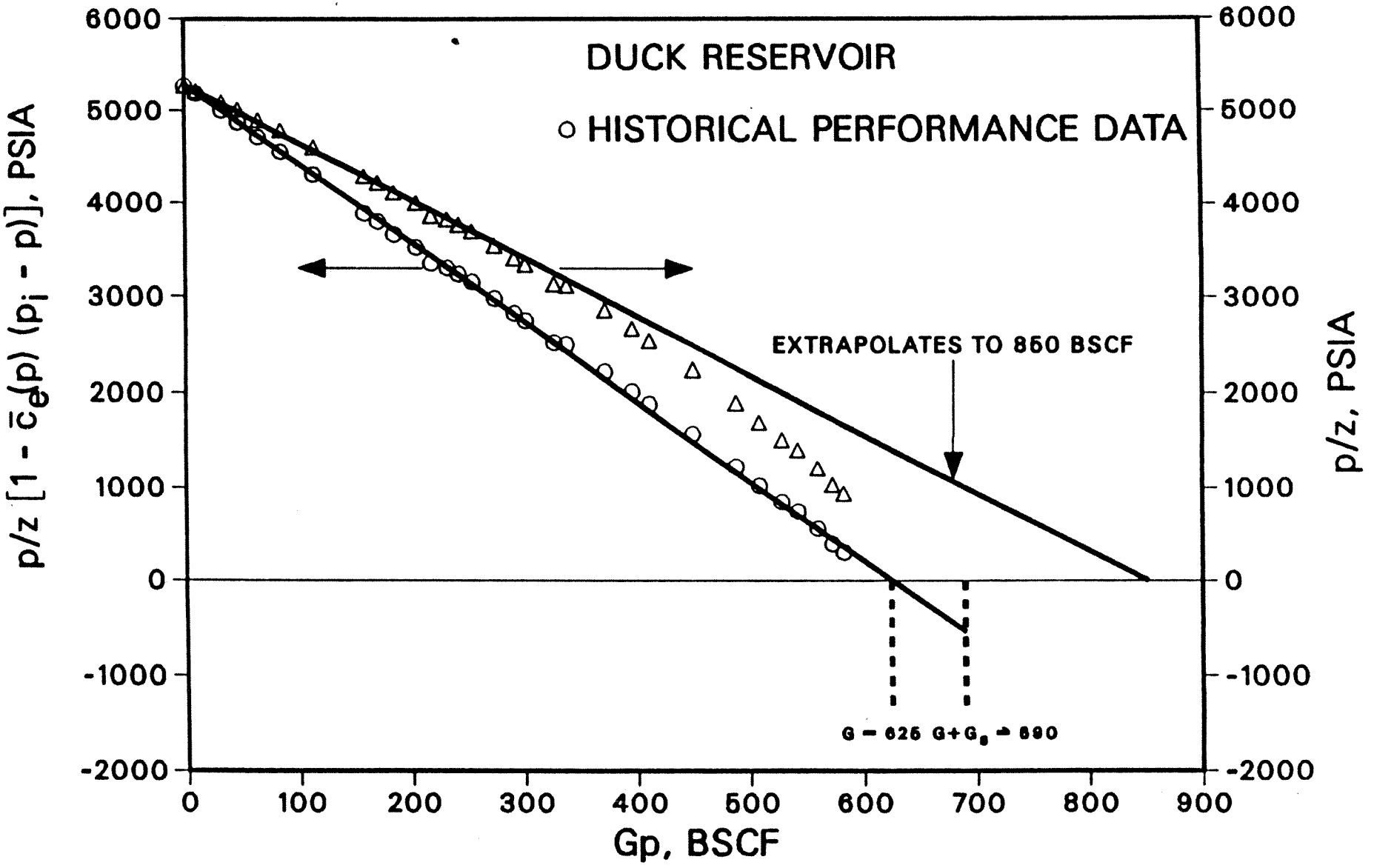

Fig. 20 Pressure vs Cumulative Production, Duck Reservoir

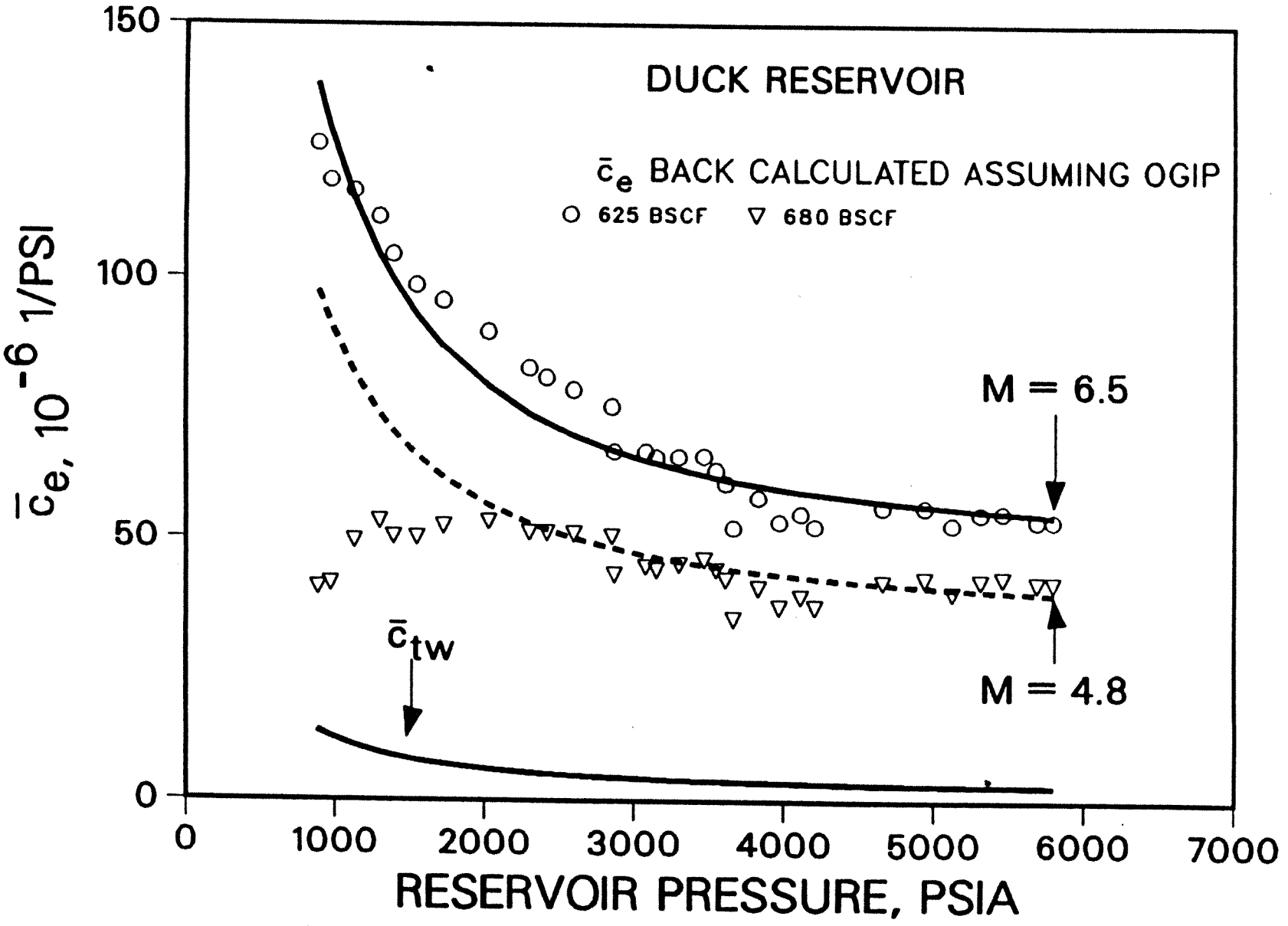

Fig. 21 Backcalculated $\bar{c}_e$ vs p at Various OGIP, Duck Reservoir

PRODUCTION / INJECTION TERMS			
G_p	G_{inj}	W_p	W_{inj}

NET RESERVOIR	ASSOCIATED WATER-BEARING VOLUMES
FREE GAS	1. *INTERBEDDED SHALES AND POOR QUALITY RESERVOIR ROCK* *(CONTAINING SOLUTION GAS)*
CONNATE WATER (CONTAINING SOLUTION GAS)	2. *LIMITED AQUIFER (CONTAINING SOLUTION GAS)*

EXTERNAL "LARGE" AQUIFER WITH TRANSIENT ENCROACHMENT BEHAVIOR

Fig. 22 General Material Balance Schematic